reported that HCV-JFH1 transfected Huh-7.5.1 cells die when all of the cells are infected and intracellular HCV RNA reaches maximum levels (Zhong et al., 2006). These findings suggest HCV-induced cytopathogenicity. However, the mechanisms have not been well documented.

In a previous study, we investigated the cellular effects of HCV infection and replication using the HCV-JFH1 cell culture system and we reported that HCV-JFH1 transfected and infected cells show substantial CPE that are characterized by massive apoptotic cell death with expression of several ER stress-induced proteins. Taking advantage of the CPE, we developed a plaque assay for HCV in cell culture and isolated subclones of HCV that showed enhanced replication and cytopathogenicity (Sekine-Osajima et al., 2008). We have demonstrated that these viral characters were determined by mutations at certain positions in the structural and nonstructural regions of the HCV genome, especially the NS5A and NS5B regions.

In this study, we investigated the mechanisms and viral nucleotide sequences involved in HCV-induced cytopathic effects using HCV-JFH1 cell culture and a newly developed cytopathic plaque-forming assay. We demonstrated that introduction of NS5A and NS5B mutations into the JFH1 clone resulted in a higher replication efficiency, although introduction of these mutations into the JFH1 subgenomic replicon has no effect on viral replication. These mutations do not affect virion entry or release of viral particles but regulate virus replication, and high levels of virus replication result in cytopathogenicity.

Results

Development of cytopathic plaques by HCV infection of Huh-7.5.1 cells

A plaque assay was performed to investigate the morphological CPE following HCV-JFH1 infection (see Materials and methods). Culture supernatants from JFH1-transfected cells were diluted serially and inoculated onto uninfected Huh-7.5.1 cells. The cells were subsequently cultured in medium containing agarose. On 9 days after the inoculation, viable cells were stained and plaques were visualized (Fig. 1A). HCV-inoculated cell cultures developed plaques as unstained areas, accompanied by rounded cells in the periphery (Fig. 1B). The formation of cytopathic plaques was not observed in a parental Huh7 cell line (data not shown). Those results were consistent with our previous study (Sekine-Osajima et al., 2008).

Introduction of mutations in the NS5A and NS5B regions of the JFH1 clone augmented its cytopathic effects

Among the amino acid substitutions that developed in the plaque-derived HCV-JFH1 strains, 6 of the 9 amino acid changes appeared redundantly among 5 independently isolated plaques, and clustered in the C terminal part of the NS5A and NS5B regions. To investigate the phenotype of each amino acid substitution, we constructed mutant JFH1

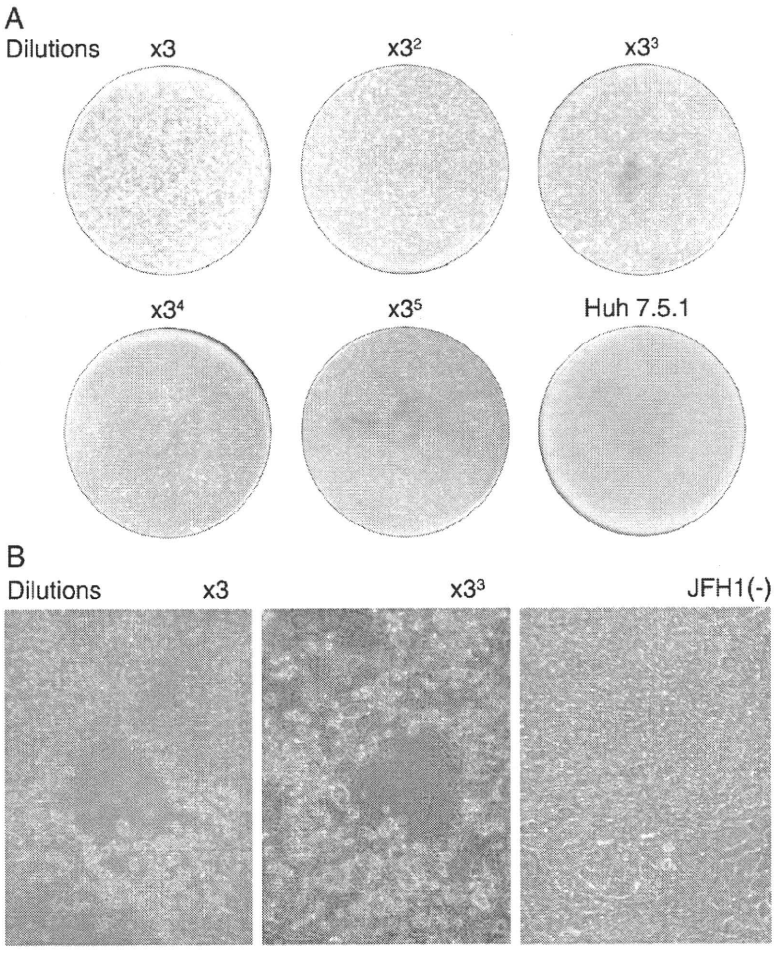

Fig. 1. The cytopathic effects of HCV-JFH1 *in vitro*. A. Plaque assay. Huh-7.5.1 cells were seeded in collagen-coated 60mm-diameter plates at density of 4×10^5 cells per plates and were incubated at 37 °C under 5.0% CO_2 (as described above). After overnight incubation, HCV-infected culture supernatants were serially diluted in a final volume of 2 ml per plates and transferred onto the cell monolayers. After ~5 h of incubation, the inocula were removed and the infected cells were overlaid with 8 ml of culture medium containing 0.8% methyl-cellulose and incubated under normal conditions. After 7 days culture, formation of cytopathic plaque was visualized by staining with 0.08% crystal violet solution. B. The cytopathic plaques were observed by phase-contrast microscopy at day 7 after HCV-JFH1 infection.

clones in which we introduced separately one amino acid substitution in NS5A and five substitutions in NS5B (Fig. 2A) and transfected the mutant HCV RNAs into Huh-7.5.1 cells. To compare the electroporation efficiencies of viral RNAs, Huh-7.5.1 cells were harvested 8 h after transfection and the levels of intracellular core antigen were measured. There was no difference in the efficiencies of electroporation (Fig. 2D). The substitutions G2964D, H3004Q, and S3005N did not lead to cytopathic effects but three mutant subclones (C2441S, P2938S and R2985P) produced much more cell death compared to the wild type JFH1 (Fig. 2B). To assess the quantitative cytopathic effect seen in host cells for each of the mutants, we also performed MTS assay at 6 days post transfection. It showed that Huh-7.5.1 cells transfected with the triple mutants (C2441S, R2938S, or R2985P) induced apparently much more cytopathic effect compared to the parental JFH1 and other mutant clones, although the three mutant clones encoding the substitutions C2441S, P2938S, or R2985P did not show significant difference but

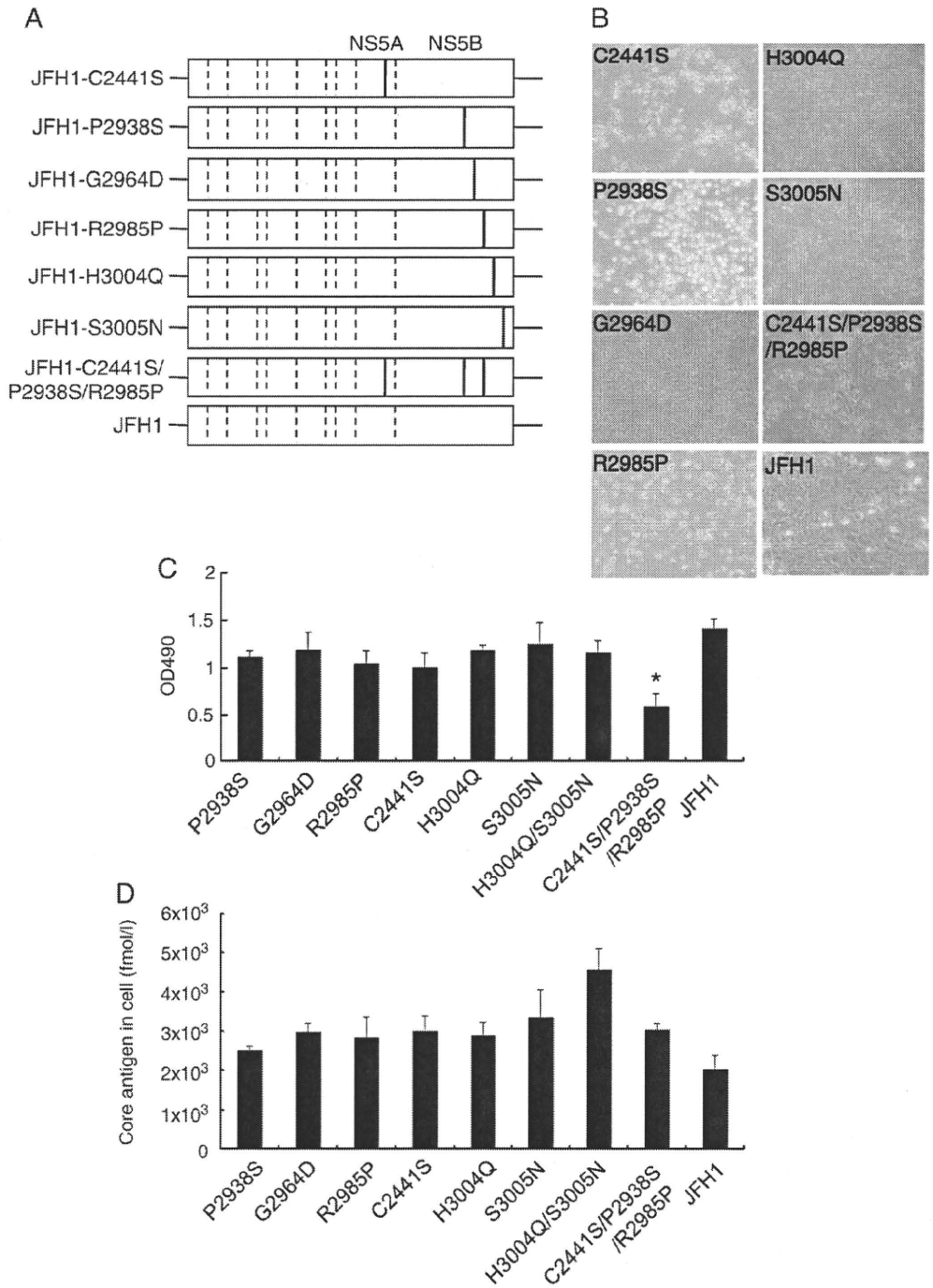

Fig. 2. Introduction of mutations into the NS5A and NS5B regions of JFH1. A. The mutations identified in the cytopathic plaque were introduced individually into the parental JFH1. Each JFH1 mutant was transfected into Huh-7.5.1 cells by electroporation. B. Huh-7.5.1 cells transfected with JFH1-mutants were observed by phase-contrast microscopy at day10 after transfection. C. MTS assay was performed to assess the quantitative cytopathic effect seen in Huh-7.5.1 cells for each of the mutants 6 days post transfection. Asterisks indicate p-values of less than 0.05 as compared with JFH1. D. Huh-7.5.1 cells were harvested at 8 h after transfection and the levels of intracellular core antigen were measured.

showed tendency to introduce more cytopathic effect than the parental JFH1 and the mutant clones encoding the substitutions G2964D, H3004Q, and S3005N (Fig. 2C).

Introduction of NS5A and NS5B mutations into the JFH1 clone led to a greater replication efficiency

To compare the expression levels of each mutant subclone, each HCV RNA was transfected and core antigen was detected subsequently in the culture medium. Similar to Fig. 2B, HCV clones with individual substitutions G2964D, H3004Q and S3005N produced significantly less core antigen or did not replicate at all. In contrast, the C2441S, P2938S and R2985P mutants produced significantly more core antigen than the wild type JFH1. In addition, an HCV clone with all 3 adaptive substitutions (C2441S, P2938S and R2985P) produced more core antigen than any other clone (Fig. 3A).

Next, we harvested the infected cells at 5 days after electroporation and performed western blotting. As shown in Fig. 3B, the three clones encoding the substitutions C2441S, P2938S, or R2985P, and the clone with all three mutations, expressed far more core protein than the parental JFH1, although the clones encoding the substitutions G2964D, H3004Q and S3005N did not express core protein. We also transferred culture media from the mutant clones onto uninfected Huh-7.5.1 cells and performed western blotting and the cells infected with the same mutant subclones as Fig. 3B expressed more core protein (Fig. 3C).

Introduction of NS5A and NS5B mutations into the JFH1 subgenomic replicon

To investigate the primary phase of replication of JFH1 mutants, we constructed JFH1 subgenomic replicons by introducing individually the six mutations in NS5A and NS5B. We transfected each replicon RNA into Huh7 cells and compared their replication levels according to the luciferase activities. Consistently with the mutant viruses, the subgenomic replicon encoding the changes C2441S, P2938S or R2985P, which produced higher amounts of core antigen, did replicate at higher levels than the other subgenomic replicons with single mutation, G2964D, H3004Q and S3005N. However, none of these mutants replicated at higher than the parental JFH1 subgenomic replicon. Furthermore, replicon with triple mutations of C2241S, P2938S and R2985P did not replicate (Fig. 4).

Introduction of NS5A and NS5B mutations into the JFH1 clone had no effect on the production of infectious virions

We sought to investigate the effects of the NS5A and NS5B mutations on virus replication and virion secretion independent of re-infection and spread of the viruses produced. Therefore, we used the S29-subclone of Huh7 cells, which cannot be infected by HCV because of a defect in CD81 expression but does support viral genomic replication and releases infectious HCV particles after transfection (Russell et al., 2008). The Huh7-S29 cells enabled us to evaluate a single cycle of infection and production of virions. Those cell lines did not show apparent cytopathic effects after transfection with HCV RNAs (data not shown). To analyze HCV particle production from cells transfected with the viral genomic RNAs transcribed in vitro, we harvested culture media and cells at 72 h post transfection and measured the core antigen levels in culture media and intracellular HCV RNA by real-time RT-PCR. The C2441S, P2938S, and R2985P mutants produced significantly greater amounts of core antigen in the culture medium than the wild type JFH1. The HCV clone carrying all three mutations produced the greatest amount of core antigen (Fig. 5A, top). Consistent with the core antigen levels in the culture media, intracellular HCV RNA levels were also higher in the cells transfected with the mutated genomes encoding separately C2441S,

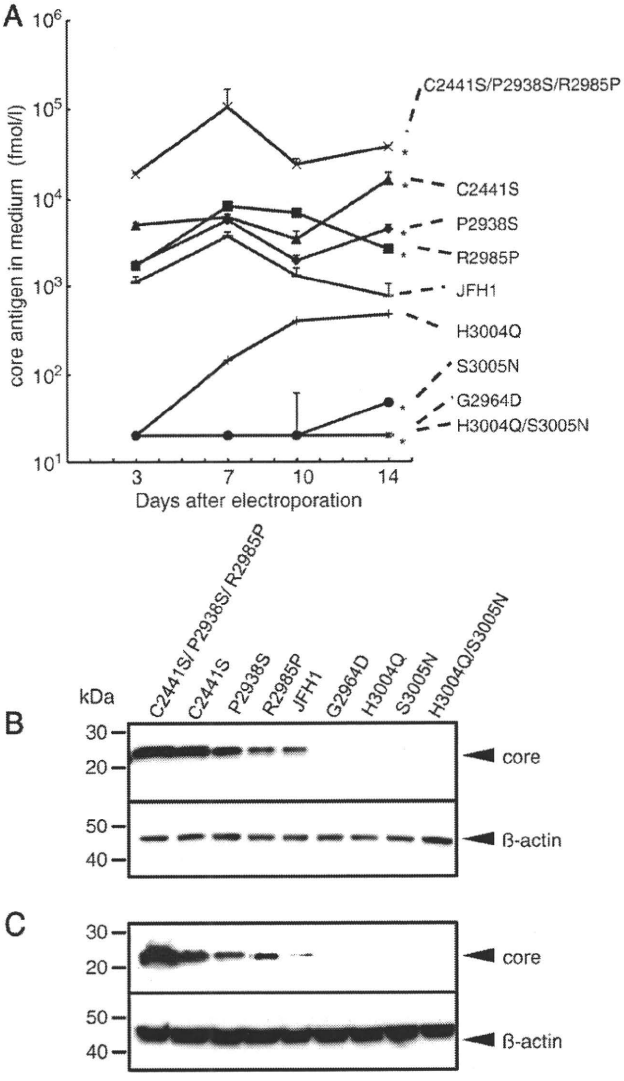

Fig. 3. Replication competences of HCV subclones with NS5A and NS5B mutations. A. Levels of core antigen in the culture medium. The culture media from transfected cells were collected on the days indicated and the levels of core antigen were measured. Asterisks indicate p-values of less than 0.05 as compared with JFH1. B. Huh-7.5.1 cells transfected with JFH1 mutants were harvested at 5 days after transfection and western blotting was performed. C. The culture media from Huh-7.5.1 cells transfected with JFH1 mutants were transferred onto uninfected Huh-7.5.1 cells. The cells were harvested at 3 days after infection. Western blotting was performed using anti-core and anti-beta-actin. kDa: kilo dalton.

P2938S, and R2985P, and that with all three mutations (Fig. 5A, middle), indicating that these mutations affected virus replication. Fig. 5A bottom shows the efficiency of infectious viral particle release from each transfectant, this being expressed as the core antigen level in the culture medium adjusted by dividing by the levels of intracellular HCV RNA. There was no difference in the efficiency of release of virions by the wild type JFH1 and the genomes carrying the C2441S, P2938S or R2985P changes. These results indicated that these three mutations in NS5A and NS5B did not affect virion entry or viral particle release but did regulate virus replication, and a high level of viral replication induces cytopathogenicity. Similarly, as shown in Fig. 3B, the three clones with C2441S, P2938S or R2985P, or all three mutations expressed much higher levels of core protein than the parental JFH1, while clones with G2964D, H3004Q or S3005N mutations did not express detectable amounts of core protein (Fig. 5B).

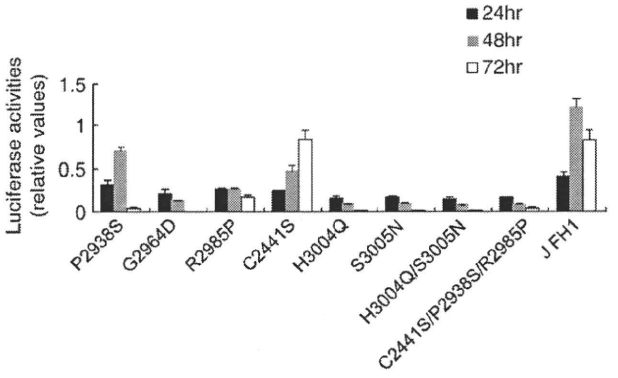

Fig. 4. Luciferase assay of the cytopathic JFH1-subgenomic replicon. Mutations were introduced into 2a-Feo subgenomic replicon and transcribed RNA for each replicon was transfected into Huh7 cells by electroporation. The cells were harvested at 24 h, 48 h and 72 h after electroporation and were used for Luciferase assay. Values are relative values to those of 8 h.

Mutations of NS5A and NS5B are associated with replication competence at earlier stages in vivo

We next used human hepatocyte chimeric mice to investigate the infectivity of the triple mutant of NS5A and NS5B. We confirmed the mouse liver chimerism greater than 70% by immunohistochemical analysis (data not shown). Culture media of the parental JFH1 and the mutant subclone with three mutations (C2441S, P2938S, and R2985P), were collected following transfection of Huh-7.5.1 cells, concentrated, and inoculated intravenously into human hepatocyte chimeric mice. We confirmed that the three mutations in NS5A and NS5B were conserved in the virus genome sequence of cell culture supernatants that were used for inoculation (data not shown). Two mice were inoculated with JFH1 and three were inoculated with the mutant virus. HCV RNA and human albumin in the sera of the mice were detected sequentially.

We repeated the same exam twice and confirmed consistency of the results. In the early phase post inoculation, the concentration of HCV RNA in serum was significantly higher in mice inoculated with the culture medium from the mutant subclone (Fig. 6A), suggesting that the mutations in NS5A and NS5B (C2441S, P2938S, and R2985P) are associated with virus replication in vivo. However, there was no difference in the level of HCV RNA in later period. The disparity of viral production at early time point could be influenced by the disparate numbers of infectious virus between the 2 initial inoculums. However, the sharp elevation of serum HCV RNA at day 5 after dropping at day 3 indicates that the mutants (C2441S, P2938S plus R2985P) are more replication competent at early stages in vivo. Serum levels of human albumin remained constant throughout the observed periods and showed no significant differences between wild and mutant-infected mice (Fig. 6B).

We also investigated expression of ER stress-related proteins, the glucose regulated protein 78 (GRP78) and C/EBP homologous protein (CHOP), in liver of chimeric mice infected with JFH1 or the mutant in the early phase post inoculation. Human hepatocyte chimeric mice were inoculated in the same way as described above, and we verified that the level of virus titer in serum of each mouse was same as presented in Fig. 6A (data not shown). We sacrificed one each mouse that was infected with wild type or mutant JFH1 at 5 day of infection and investigated hepatic expression of GRP78 and CHOP. Liver histology showed no sign of inflammation or cytopathic cell death. However, as shown in Fig. 7, the expression level of both GRP78 and CHOP was higher in mice inoculated with the mutant viruses than the parental JFH1. There was no apparent difference in percents of hepatic chimerism between each mouse. These finding suggested that ER stress-related proteins were upregulated in the liver of HCV-infected mouse and that these responses were more strongly induced in the liver of mutant-infected mouse.

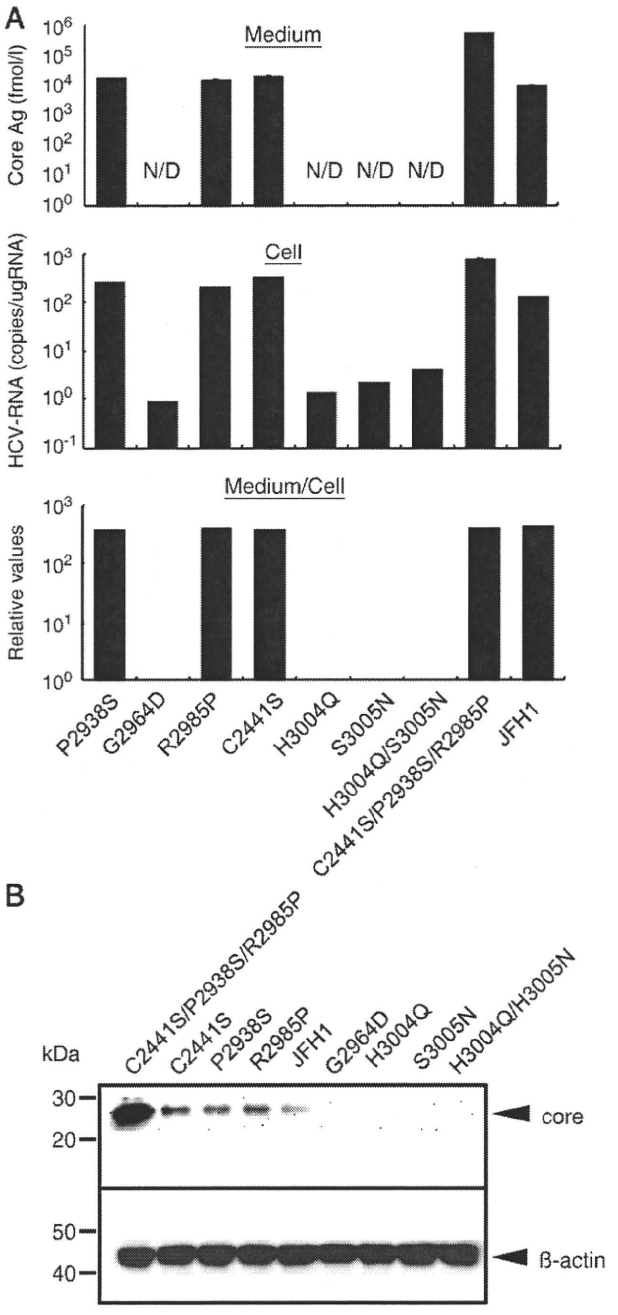

Fig. 5. Analysis of viral replication and production of viral particles using a single-cycle assay. A. Levels of core antigen in the culture media 3 days after transfection of JFH1 mutants into CD81-deficient Huh7-S29 cells (top). Levels of intracellular HCV RNA were quantified by real-time RT-PCR 3 days after transfection of JFH1 mutants into Huh7-S29 cells (middle). To determine the efficiency of infectious viral particle release from Huh7-S29 cells transfected with JFH1 mutants, the levels of core antigen in the culture media were adjusted by dividing by the levels of intracellular HCV RNA (bottom). Core Ag: Core antigen, N/D: not detectable. B. Huh7-S29 cells were harvested at 3 days after transfection of JFH1 mutants and western blotting was performed using anti-core and anti-beta-actin. kDa: kilo dalton.

Highly adapted cytopathic mutations reverted to wild type in vivo

Finally, we analyzed the serum viral sequence at the specified time points. On days 1 and 5, the HCV genomic sequences of the mice

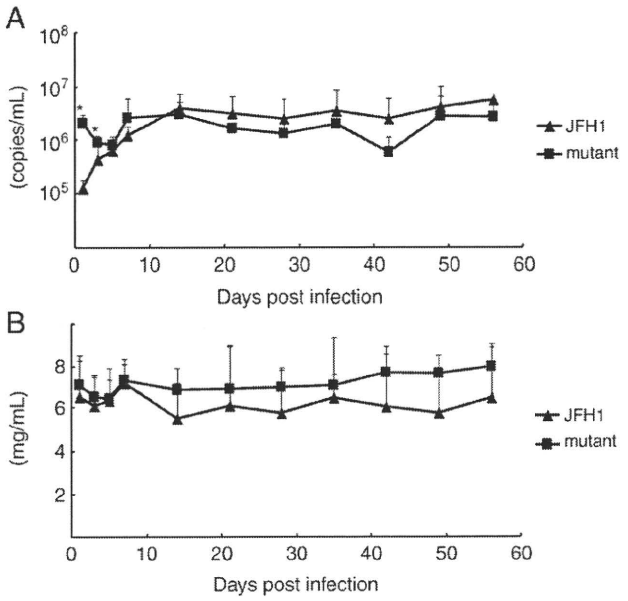

Fig. 6. In vivo analysis of cytopathic JFH1 mutants using human hepatocyte chimeric mice. A. Serial changes in HCV RNA in the sera of mice inoculated with the culture media from JFH1 mutants. The data shows the average of 2 mice for JFH1, and 3 mice for the mutant. Asterisks indicate p-values of less than 0.05 as compared with JFH1. B. Levels of human albumin in the sera of mice inoculated with the culture media from JFH1 mutants.

inoculated with the cytopathic mutant virus showed conservation of the mutations in codons 2441, 2938 and 2985. However, on days 21 and later, the mutation at codon 2985 had reverted to the wild type JFH1 sequence in all the mutant-injected mice and the mutation at codon 2938 had reverted to the wild type JFH1 sequence in two of the three mice. The C2441S mutation was more stable in the mutant-injected mice, but one mouse had lost it at day 56 (Fig. 8).

Discussion

In this study, we investigated the significance of genetic mutations in plaque-purified, cytopathic HCV-JFH1 subclones. Genetically engineered JFH1-mutants encoding C2441S, P2938S, and R2985P led to much more cell death than the wild type JFH1, and also produced significantly higher amounts of core antigen in the culture medium and inside the cells than the parental JFH1 clone. In the single-cycle production assay, which exploited a receptor-deficient Huh7 cell line, the three JFH1-mutants, JFH1-C2441S, P2938S, and R2985P produced significantly more core antigen in the culture medium and expressed equivalently higher amounts of viral genomic RNA in the cells. These data suggest that the three mutations in NS5A and NS5B (C2441S, P2938S, and R2985P) are associated directly with enhanced intracellular replication and resultant virion formation, which correlated with the extent of the cytopathic effects. Interestingly, inoculation of a cytopathogenic mutant, JFH1-C2441S/P2938S/R2985P, into human hepatocyte chimeric mice produced significantly higher plasma HCV RNA concentrations than JFH1 at ~7 days post inoculation. At a later phase of infection, however, the mutations in this mutant HCV reverted partially to the wild type sequences. Taking all things together, it is suggested that in vitro-isolated, genetically modified cytopathic HCV subclones replicate robustly in the acute phase of in vivo infection but are eliminated rapidly and substituted by in vivo adapted clones.

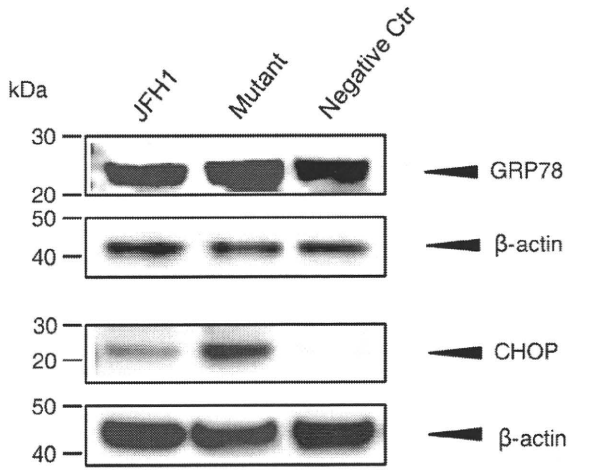

Fig. 7. Expression of ER stress-related proteins in human hepatocytes of chimeric mice infected with JFH1 or the mutant in the early phase. Western-blot analysis of the liver tissues of infected chimeric mice using anti-GRP78 goat monoclonal antibody, anti-GADD153/CHOP rabbit polyclonal antibody and anti-beta-actin. Liver samples were obtained at 5 days after inoculation. The negative control liver samples for this study was from uninfected human hepatocyte chimeric mouse.

Four of the five NS5B mutations appeared independently in several isolated subclones. This made us speculate that these amino acid substitutions may affect the enzymatic activity of RdRp. Mapping of the amino acid substitutions in the RdRp tertiary structure revealed that amino acid 2441 is located on the finger domain, and three amino acids, 2938, 2964, and 2985, are on the outer surface of the thumb domain, which corresponds to the opposite side of the nucleotide tunnel. The other substitutions, 3004 and 3005, are within the domain of the polypeptide linking the polymerase to the membrane anchor (Lesburg et al., 1999). Our preliminary study has shown that the NS5B mutations, P2938S and R2985P, did not affect cell-free enzymatic activities of the RNA polymerase. Thus, it is speculated that these mutations may affect the stability of the HCV replicase complex by altering surface affinity to other nonstructural proteins.

There are several reports on cell culture adaptive mutations in the HCV-JFH1 genome that gave more vigorous and consistent virus expression. Most studies involved prolonged cell culture of HCV-JFH1 or multiple rounds of successive passage onto naïve cells. Zhong et al. detected the E2-G451R mutation after culture for more than 60 days. The mutation led to more efficient production of infectious viral particles than wild type JFH1 (Zhong et al., 2006). Delgrange et al. conducted successive virus infections of naïve cells and identified the E2-N534K mutation that facilitated virus-CD81 attachment, and core-F172C and -P173S that increased secretion of virions (Delgrange et al., 2007). Using a similar method, Russell et al. identified E2-N417S that improved virus–cell attachment, and p7-N765D and NS2-Q1012R that increased virion production (Russell et al., 2008). Kaul et al. reported the NS5A-V2440L mutation, that was close to the C terminus and increased virion production (Kaul et al., 2007). Yi et al. used a chimeric virus of genotype 1a and JFH1 and identified the NS3-Q1251L mutation that resulted in enhanced virus production, possibly through improved interactions between NS2 and NS3 that were required for virion formation (Yi et al., 2002). Han et al. used EGFP-tagged virus and identified the mutually dependent mutations, NS3-M1290K and NS5A-T2438I, which improved virus production synergistically (Han et al., 2009).

Of note is that all of the mutations reported above promoted virion secretion or virus–cell surface interaction and none of them showed any effect on intracellular replication of viral RNA or translation of virus proteins. None of the adaptive mutations reported above overlapped with our cytopathogenic mutations. The mutations that we have identified conferred enhanced virus replication and protein expression in the early/acute stages of infection and subsequently led to massive cell death. Our data and the reports of other groups suggest that the HCV genome evolves to adapt to the host cell environment. Mutations that optimize virus secretion or virus–cell entry may be

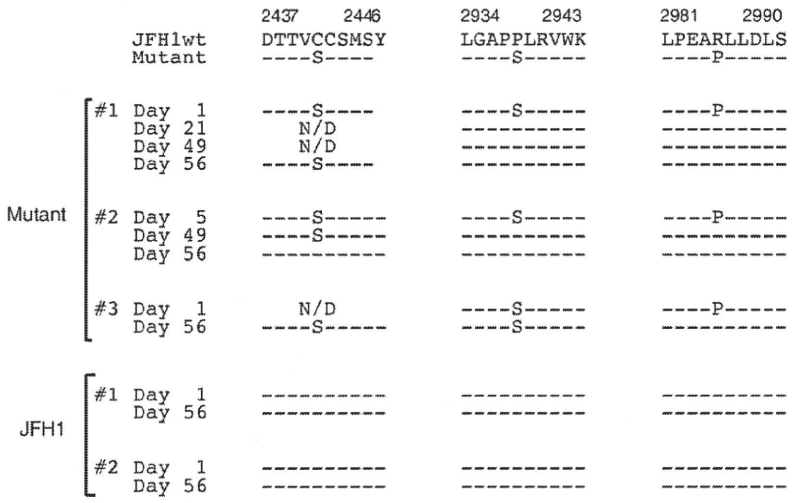

Fig. 8. Nucleotide sequence analysis of virus genomes circulating in the sera of infected mice. We extracted RNA from the sera of mice inoculated with culture media from JFH1 or JFH1-mutants and analyzed the viral sequence at the specified time points. N/D is not detectable. Wt: Wild type.

required for persistent infection in vitro, while those that affect cellular viral RNA replication may possibly promote viral genetic evolution and host cell damage.

The results of in vivo experiments using human hepatocyte chimeric mice were consistent with those of virus cell culture (Figs. 5, 6 and 7). The mutant JFH1 clones showed markedly higher levels of replication than the parental JFH1 in the acute phases. However, the serum HCV titers subsequently leveled out after two weeks of infection, concomitant with reversal of some cytopathic mutations to wild type sequences. Bukh et al. reported that inoculation of the HCV-1b genome into chimpanzee liver resulted in persistent infection, although the mutation reverted rapidly to wild type (Bukh et al., 2002). In this study, the NS5A-C2441S mutation was preserved in 2 of 3 mice, while NS5B-P2938S reverted to the wild type sequences in 2 of 3 mice and NS5B-R2985P reverted to wild type sequences in all 3 mice. These results suggest that the highly adapted JFH1 genome is infectious and viable in vivo, but is not as fit in vitro.

It is not clear why the subgenomic replicons with C2441S, P2938S or R2985P mutations did not show differences in replication levels compared to the wild type JFH1 subgenomic replicon. One may speculate that this discrepancy between the results using full-length HCV genomes and replicons might be the presence or absence of the HCV structural proteins. In addition, three individual substitutions G2964D, H3004Q and S3005N did not enhance viral replication as compared with the parental JFH1 nor did express detectable amounts of core protein. It is speculated that these mutants exist in host cells through co-infection with replication-competent viral clones resulting in enhanced replication.

There is clinical evidence that suggests the pathological outcomes of hepatitis C result from the immune response of the host rather than the direct cytopathic effects of the virus (Cerny and Chisari, 1999). However, several clinical studies have shown that fulminant hepatic failure (FHF, the HCV-JFH1 strain was isolated from such a case) featured massive hepatocyte apoptosis, as characterized by caspase activation and Fas–FasL expression (Leifeld et al., 2006; Mita et al., 2005; Ryo et al., 2000). The ER stress markers, GRP78 and ATF6 are upregulated in HCV-infected liver tissue as the histological grade advances (Shuda et al., 2003). This background and our results in vitro and in vivo suggest that HCV strains with highly infectious and cytopathic gene signatures may replicate aggressively in the acute phase of infection and that certain defects in innate or adaptive immune responses against the virus could lead to severe and persistent liver damage due to cytopathic effects induced directly by HCV. Such mechanisms might explain some rare clinical features of HCV infection, such as fulminant hepatic failure and post-transplantation severe fibrosing cholestatic hepatitis (Delladetsima et al., 1999; Dixon and Crawford, 2007).

In conclusion, we identified three substitutions in cytopathic HCV-JFH1 subclones derived from plaque assay. These substitutions directly enhanced virus replication in the early phases of virus infection in vitro and in vivo. This highly enhanced replication induced ER stress-mediated apoptosis and resulted in cytopathogenicity. Further analyses of cellular effects on HCV replication may elucidate the pathogenesis of HCV infection and may define novel host factors as targets of antiviral chemotherapeutics.

Materials and methods

Cells and cell culture

Huh-7.5.1 cells (Zhong et al., 2005) (kindly provided by Dr Francis V. Chisari) and CD81 deficient Huh7-S29 cells (Russell et al., 2008) (kindly provided by Dr Rodney S. Russell and Dr Robert H. Purcell) were maintained in Dulbecco's modified minimal essential medium (DMEM, Sigma, St. Louis, MO) supplemented with 2 mmol/L L-glutamine and 10% fetal bovine serum at 37 °C under 5.0% CO_2.

Sequence analysis

The cDNA from the isolated JFH1-plaque was amplified from cytopathic virus-infected Huh-7.5.1 cells by RT-PCR and subjected to direct sequencing.

In vitro RNA synthesis and transfection

A plasmid, pJFH1full (Wakita et al., 2005), which encodes full-length HCV-JFH1 sequence, was used. In vitro RNA synthesis and transfection were conducted as previously described (Sekine-Osajima et al., 2008). Briefly, HCV RNA was synthesized from linearized pJFH1 plasmid as template and transfected into Huh-7.5.1 cells by electroporation. The transfected cells were split every 3 to 5 days. The culture media were subsequently transferred onto uninfected Huh-7.5.1 cells and Huh7-S29 cells. The levels of HCV replication and viral protein expression were detected by real-time PCR and western blotting.

Plaque assay

HCV plaque assays were performed as reported previously (Sekine-Osajima et al., 2008). Huh-7.5.1 cells were seeded in collagen-coated 60 mm-diameter plates. After overnight incubation, HCV-infected culture media were serially diluted in a final volume of 2 ml per plate and transferred onto the cell monolayer. After ~5 h of incubation, the inocula were removed and the cell monolayer was overlaid with 8 ml of culture medium containing 0.8% methylcellulose (Sigma). After 7 to 12 days culture, cytopathic plaques were visualized by staining with 0.08% crystal violet solution (Sigma). The levels of cytotoxicity were evaluated by counting the plaques and calculating the titer (plaque-forming unit/ml).

Establishment of mutant JFH1 clones

In order to introduce various mutations into the NS5A and NS5B region of JFH1, plasmid pJFH1 was digested with HindIII and the DNA fragment encompassing nt. 8231 to 9731 was subcloned into the pBluescript II SK+ phagemid vector (Stratagene, La Jolla, CA). Mutations were introduced into the DNA fragment in the subcloning vector by site-directed mutagenesis (Quick-ChangeII Site-Directed Mutagenesis Kit, Stratagene) to generate the following codon changes: P2938S, G2964D, R2985P, H3004Q and S3005N. Finally, the HindIII–HindIII fragments were subcloned back into the parental plasmid, pJFH1. A PCR fragment (nt. 7421–7839) was subcloned into the pGEM-T Easy plasmid vector (Promega, Madison, WI) and digested with RsrII and BsrGI. Finally, after introducing the codon change C2441S, the RsrII–BsrGI fragment was reinserted into the parental plasmid.

Quantification of HCV core antigen in the culture medium

The culture media from JFH1-RNA transfected Huh-7.5.1 cells and Huh7-S29 cells were collected on the days indicated, passed through a 0.45 μm filter (MILLEX-HA, Millipore, Bedford, MA), and stored at −80 °C. The levels of core antigen in the culture media were measured using a chemiluminescence enzyme immunoassay (CLEIA) according to the manufacturer's protocol (Lumipulse Ortho HCV Antigen, Ortho-Clinical Diagnostics, Tokyo, Japan).

Western blotting

Western blotting was carried out as described previously (Itsui et al., 2009). Briefly, 10 μg of total cell lysate were separated by SDS-PAGE and blotted onto a polyvinylidene fluoride (PVDF) Western Blotting membrane. The membrane was incubated with the primary antibodies followed by a peroxidase-labeled anti IgG antibody, and visualized by chemiluminescence using the ECL Western blotting Analysis System (Amersham Bioscience, Buckinghamshire, UK). The antibodies used were anti-core mouse monoclonal antibody (Abcam, Cambridge, MA), anti-GRP78 goat monoclonal antibody, anti-GADD153/CHOP rabbit polyclonal antibody (Santa Cruz Biotechnology, Santa Cruz, CA), and anti-beta-actin antibody (Sigma).

HCV subgenomic replicon constructs

The HCV subgenomic replicon plasmid, pRep-Feo, was derived from the HCV-N strain, pHCV1bneo-delS (Tanabe et al., 2004; Yokota et al., 2003). The replicon RNA was synthesized from pRep-Feo and transfected into Huh7 cells.

Luciferase reporter assay

Luciferase activity was measured using a 1420 Multilabel Counter (ARVO MX, Perkin Elmer, Waltham, MA) with a Bright-Glo Luciferase Assay System (Promega) (Tasaka et al., 2007). Assays were carried out in triplicate and the results expressed as means ± SD.

MTS assays

To evaluate cell viability, dimethylthiazol carboxymethoxy-phenyl sulfophenyl tetrazolium (MTS) assays were performed using a CellTiter 96 Aqueous One Solution Cell Proliferation Assay kit (Promega), as described previously (Sakamoto et al., 2007).

Real-time RT-PCR analysis

Total cellular RNA was isolated using an RNeasy Mini Kit (QIAGEN, Valencia, CA). Two micro-grams of total cellular RNA were used to generate cDNA from each sample using SuperScript II (Invitrogen) reverse transcriptase. Expression of mRNA was quantified using TaqMan Universal PCR Master Mix (Applied Biosystems) and the ABI 7500 Real-Time PCR System (Applied Biosystems). The primers used were as follows: HCV-JFH1 sense (positions 285 to 307; 5′-GGTACTGCCTGATAGGGTGCTT-3′), HCV-JFH1 antisense (positions 349 to 375; 5′-TGGTTTTTCTTTGAGGTTTAGGATTC-3′), GAPDH sense (5′-CCTCCCGCTTCGCTCTCT-3′), and GAPDH antisense (5′-GCTGGCGACGCAAAAGA-3′).

HCV RNA inoculation into human hepatocyte chimeric mice

Housing, maintenance, and care of the mice used in this study conformed to the requirement for the humane use of animals in scientific research as defined by Animal Care and Use Committee of our institute. The culture media of Huh-7.5.1 cells transfected with parental JFH1 and JFH1 mutants were collected 10 days after transfection and passed through a 0.45 μm filter. The three mutations introduced in NS5A and NS5B were confirmed to conserve by the sequence analysis of virus genome of cell culture supernatants before inoculation. Filtrated culture medium was then pooled and concentrated using Amicon Ultra-15 (100,000 molecular weight cutoff, Millipore). 100 μl of each culture medium was injected intravenously into human hepatocyte chimeric mice (PXB mice, Phenix Bio, Hiroshima, Japan) (Mercer et al., 2001). The rate of liver chimerism of these human hepatocyte chimeric mice was confirmed more than 70% by immunohistochemical analysis. After infection, blood samples were taken serially and levels for HCV RNA and human albumin were quantified using real-time RT-PCR and an enzyme immunoassay, respectively. RNA was extracted from serum samples and subjected to direct sequence determination.

Protein extraction from human hepatocyte chimeric mice and expression of ER stress-related proteins

5 days post inoculation, mice were sacrificed and proteins were extracted from liver samples with complete Lysis-M Reagent Kit (Roche Applied Science, Indianapolis, IN). One Mini Protease Inhibitor Cocktail Tablet was dissolved into 10 ml of Lysis-M Reagent and 500 μl of this fluid was added to 50 μg of each liver sample and homogenized. The lysate was transferred to a microcentrifuge tube and centrifuged at 14,000×*g* for 5 min. The supernatant containing soluble protein was transferred to a new reaction tube and 20 μg of each protein was used for western blotting to detect ER stress-related proteins.

Acknowledgments

We are indebted to Dr. Francis V. Chisari for providing the Huh-7.5.1 cell line and Dr. Rodney S. Russell for receptor-deficient Huh7-S29 cells. This study was supported by grants from Ministry of Education, Culture, Sports, Science and Technology-Japan, the Japan Society for the Promotion of Science, Ministry of Health, Labour and

Welfare-Japan, Japan Health Sciences Foundation, and National Institute of Biomedical Innovation.

References

Alter, M.J., 1997. Epidemiology of hepatitis C. Hepatology 26, 62S–65S.

Bartenschlager, R., Lohmann, V., 2000. Replication of hepatitis C virus. J. Gen. Virol. 81, 1631–1648.

Bukh, J., Pietschmann, T., Lohmann, V., Krieger, N., Faulk, K., Engle, R.E., Govindarajan, S., Shapiro, M., Claire, M.S., Bartenschlager, R., 2002. Mutations that permit efficient replication of hepatitis C virus RNA in Huh-7 cells prevent productive replication in chimpanzees. Proc. Natl. Acad. Sci. U. S. A. 99 (22), 14416–14421.

Cerny, A., Chisari, F.V., 1999. Pathogenesis of chronic hepatitis C: immunological features of hepatic injury and viral persistence. Hepatology 30 (3), 595–601.

Delgrange, D., Pillez, A., Castelain, S., Cocquerel, L., Rouille, Y., Dubuisson, J., Wakita, T., Duverlie, G., Wychowski, C., 2007. Robust production of infectious viral particles in Huh-7 cells by introducing mutations in hepatitis C virus structural proteins. J. Gen. Virol. 88 (Pt 9), 2495–2503.

Delladetsima, J.K., Boletis, J.N., Makris, F., Psichogiou, M., Kostakis, A., Hatzakis, A., 1999. Fibrosing cholestatic hepatitis in renal transplant recipients with hepatitis C virus infection. Liver Transpl. Surg. 5 (4), 294–300.

Dixon, L.R., Crawford, J.M., 2007. Early histologic changes in fibrosing cholestatic hepatitis C. Liver Transpl. 13 (2), 219–226.

Fried, M.W., Shiffman, M.L., Reddy, K.R., Smith, C., Marionos, G., Goncales, F.L., Häussinger, D., Diago, M., Garosi, G., Dhumeaux, D., Craxi, A., Lin, A., Hoffman, J., Yu, J., 2002. Peginterferon alfa-2a plus ribavirin for chronic hepatitis C virus infection. N. Engl. J. Med. 347, 975–982.

Han, Q., Xu, C., Wu, C., Zhu, W., Yang, R., Chen, X., 2009. Compensatory mutations in NS3 and NS5A proteins enhance the virus production capability of hepatitis C reporter virus. Virus Res. 145 (1), 63–73.

Itsui, Y., Sakamoto, N., Kakinuma, S., Nakagawa, M., Sekine-Osajima, Y., Tasaka-Fujita, M., Nishimura-Sakurai, Y., Suda, G., Karakama, Y., Yamamoto, M., Watanabe, T., Ueyama, M., Funaoka, Y., Azuma, S., and Watanabe, M. (2009). Antiviral effects of the interferon-induced protein GBP-1 and its interaction with the hepatitis C virus NS5B protein. Hepatology 50 (6), 1727–1737.

Jordan, R., Wang, L., Graczyk, T.M., Block, T.M., Romano, P.R., 2002. Replication of a cytopathic strain of bovine viral diarrhea virus activates PERK and induces endoplasmic reticulum stress-mediated apoptosis of MDBK cells. J. Virol. 76 (19), 9588–9599.

Kato, N., 2001. Molecular virology of hepatitis C virus. Acta Med. Okayama 55 (3), 133–159.

Kato, T., Date, T., Miyamoto, M., Furusaka, A., Tokushige, K., Mizokami, M., Wakita, T., 2003. Efficient replication of the genotype 2a hepatitis C virus subgenomic replicon. Gastroenterology 125 (6), 1808–1817.

Kaul, A., Woerz, I., Meuleman, P., Leroux-Roels, G., Bartenschlager, R., 2007. Cell culture adaptation of hepatitis C virus and in vivo viability of an adapted variant. J. Virol. 81 (23), 13168–13179.

Koutsoudakis, G., Herrmann, E., Kallis, S., Bartenschlager, R., Pietschmann, T., 2007. The level of CD81 cell surface expression is a key determinant for productive entry of hepatitis C virus into host cells. J. Virol. 81 (2), 588–598.

Leifeld, L., Nattermann, J., Fielenbach, M., Schmitz, V., Sauerbruch, T., Spengler, U., 2006. Intrahepatic activation of caspases in human fulminant hepatic failure. Liver Int. 26 (7), 872–879.

Lesburg, C.A., Cable, M.B., Ferrari, E., Hong, Z., Mannarino, A.F., Weber, P.C., 1999. Crystal structure of the RNA-dependent RNA polymerase from hepatitis C virus reveals a fully encircled active site. Nat. Struct. Biol. 6 (10), 937–943.

Lindenbach, B.D., Evans, M.J., Syder, A.J., Wolk, B., Tellinghuisen, T.L., Liu, C.C., Maruyama, T., Hynes, R.O., Burton, D.R., McKeating, J.A., Rice, C.M., 2005. Complete replication of hepatitis C virus in cell culture. Science 309 (5734), 623–626.

Lohmann, V., Korner, F., Koch, J., Herian, U., Theilmann, L., Bartenschlager, R., 1999. Replication of subgenomic hepatitis C virus RNAs in a hepatoma cell line. Science 285 (5424), 110–113.

Mercer, D.F., Schiller, D.E., Elliott, J.F., Douglas, D.N., Hao, C., Rinfret, A., Addison, W.R., Fischer, K.P., Churchill, T.A., Lakey, J.R., Tyrrell, D.L., Kneteman, N.M., 2001. Hepatitis C virus replication in mice with chimeric human livers. Nat. Med. 7 (8), 927–933.

Mita, A., Hashikura, Y., Tagawa, Y., Nakayama, J., Kawakubo, M., Miyagawa, S., 2005. Expression of Fas ligand by hepatic macrophages in patients with fulminant hepatic failure. Am. J. Gastroenterol. 100 (11), 2551–2559.

Mottola, G., Cardinali, G., Ceccacci, A., Trozzi, C., Bartholomew, L., Torrisi, M.R., Pedrazzini, E., Bonatti, S., Migliaccio, G., 2002. Hepatitis C virus nonstructural proteins are localized in a modified endoplasmic reticulum of cells expressing viral subgenomic replicons. Virology 293 (1), 31–43.

Russell, R.S., Meunier, J.C., Takikawa, S., Faulk, K., Engle, R.E., Bukh, J., Purcell, R.H., Emerson, S.U., 2008. Advantages of a single-cycle production assay to study cell culture-adaptive mutations of hepatitis C virus. Proc. Natl. Acad. Sci. U. S. A. 105 (11), 4370–4375.

Ryo, K., Kamogawa, Y., Ikeda, I., Yamauchi, K., Yonehara, S., Nagata, S., Hayashi, N., 2000. Significance of Fas antigen-mediated apoptosis in human fulminant hepatic failure. Am. J. Gastroenterol. 95 (8), 2047–2055.

Sakamoto, N., Watanabe, M., 2009. New therapeutic approaches to hepatitis C virus. J. Gastroenterol. 44 (7), 643–649.

Sakamoto, N., Yoshimura, M., Kimura, T., Toyama, K., Sekine-Osajima, Y., Watanabe, M., Muramatsu, M., 2007. Bone morphogenetic protein-7 and interferon-alpha synergistically suppress hepatitis C virus replicon. Biochem. Biophys. Res. Commun. 357 (2), 467–473.

Sekine-Osajima, Y., Sakamoto, N., Mishima, K., Nakagawa, M., Itsui, Y., Tasaka, M., Nishimura-Sakurai, Y., Chen, C.H., Kanai, T., Tsuchiya, K., Wakita, T., Enomoto, N., Watanabe, M., 2008. Development of plaque assays for hepatitis C virus-JFH1 strain and isolation of mutants with enhanced cytopathogenicity and replication capacity. Virology 371 (1), 71–85.

Shuda, M., Kondoh, N., Imazeki, N., Tanaka, K., Okada, T., Mori, K., Hada, A., Arai, M., Wakatsuki, T., Matsubara, O., Yamamoto, N., Yamamoto, M., 2003. Activation of the ATF6, XBP1 and grp78 genes in human hepatocellular carcinoma: a possible involvement of the ER stress pathway in hepatocarcinogenesis. J. Hepatol. 38 (5), 605–614.

Tanabe, Y., Sakamoto, N., Enomoto, N., Kurosaki, M., Ueda, E., Maekawa, S., Yamashiro, T., Nakagawa, M., Chen, C.H., Kanazawa, N., Watanabe, M., 2004. Synergistic inhibition of intracellular hepatitis C virus replication by combination of ribavirin and interferon-alpha. J. Infect. Dis. 189, 1129–1139.

Tasaka, M., Sakamoto, N., Itakura, Y., Nakagawa, M., Itsui, Y., Sekine-Osajima, Y., Nishimura-Sakurai, Y., Chen, C.H., Yoneyama, M., Fujita, T., Wakita, T., Maekawa, S., Enomoto, N., Watanabe, M., 2007. Hepatitis C virus non-structural proteins responsible for suppression of the RIG-I/Cardif-induced interferon response. J. Gen. Virol. 88 (Pt 12), 3323–3333.

Wakita, T., Pietschmann, T., Kato, T., Date, T., Miyamoto, M., Zhao, Z., Murthy, K., Habermann, A., Krausslich, H.G., Mizokami, M., Bartenschlager, R., Liang, T.J., 2005. Production of infectious hepatitis C virus in tissue culture from a cloned viral genome. Nat. Med. 11 (7), 791–796.

Yi, M., Bodola, F., Lemon, S.M., 2002. Subgenomic hepatitis C virus replicons inducing expression of a secreted enzymatic reporter protein. Virology 304 (2), 197–210.

Yokota, T., Sakamoto, N., Enomoto, N., Tanabe, Y., Miyagishi, M., Maekawa, S., Yi, L., Kurosaki, M., Taira, K., Watanabe, M., Mizusawa, H., 2003. Inhibition of intracellular hepatitis C virus replication by synthetic and vector-derived small interfering RNAs. EMBO Rep. 4 (6), 602–608.

Zhong, J., Gastaminza, P., Cheng, G., Kapadia, S., Kato, T., Burton, D.R., Wieland, S.F., Uprichard, S.L., Wakita, T., Chisari, F.V., 2005. Robust hepatitis C virus infection in vitro. Proc. Natl. Acad. Sci. U. S. A. 102 (26), 9294–9299.

Zhong, J., Gastaminza, P., Chung, J., Stamataki, Z., Isogawa, M., Cheng, G., McKeating, J.A., Chisari, F.V., 2006. Persistent hepatitis C virus infection in vitro: coevolution of virus and host. J. Virol. 80 (22), 11082–11093.

RNA Polymerase Activity and Specific RNA Structure Are Required for Efficient HCV Replication in Cultured Cells

Asako Murayama[1☯], Leiyun Weng[2☯], Tomoko Date[1], Daisuke Akazawa[1,3], Xiao Tian[2], Tetsuro Suzuki[1], Takanobu Kato[1], Yasuhito Tanaka[4], Masashi Mizokami[5], Takaji Wakita[1*], Tetsuya Toyoda[2*]

1 Department of Virology II, National Institute of Infectious Diseases, Tokyo, Japan, **2** Unit of Viral Genome Regulation, Key Laboratory of Molecular Virology & Immunology, Institute Pasteur of Shanghai, Chinese Academy of Sciences, Shanghai, People's Republic of China, **3** Pharmaceutical Research Lab, Toray Industries, Inc., Kanagawa, Japan, **4** Department of Clinical Molecular Informative Medicine, Nagoya City University Graduate School of Medical Sciences, Aichi, Japan, **5** Research Center for Hepatitis and Immunology, Kohnodai Hospital, International Medical Center of Japan, Chiba, Japan

Abstract

We have previously reported that the NS3 helicase (N3H) and NS5B-to-3'X (N5BX) regions are important for the efficient replication of hepatitis C virus (HCV) strain JFH-1 and viral production in HuH-7 cells. In the current study, we investigated the relationships between HCV genome replication, virus production, and the structure of N5BX. We found that the Q377R, A450S, S455N, R517K, and Y561F mutations in the NS5B region resulted in up-regulation of J6CF NS5B polymerase activity *in vitro*. However, the activation effects of these mutations on viral RNA replication and virus production with JFH-1 N3H appeared to differ. In the presence of the N3H region and 3' untranslated region (UTR) of JFH-1, A450S, R517K, and Y561F together were sufficient to confer HCV genome replication activity and virus production ability to J6CF in cultured cells. Y561F was also involved in the kissing-loop interaction between SL3.2 in the NS5B region and SL2 in the 3'X region. We next analyzed the 3' structure of HCV genome RNA. The shorter polyU/UC tracts of JFH-1 resulted in more efficient RNA replication than J6CF. Furthermore, 9458G in the JFH-1 variable region (VR) was responsible for RNA replication activity because of its RNA structures. In conclusion, N3H, high polymerase activity, enhanced kissing-loop interactions, and optimal viral RNA structure in the 3'UTR were required for J6CF replication in cultured cells.

Citation: Murayama A, Weng L, Date T, Akazawa D, Tian X, et al. (2010) RNA Polymerase Activity and Specific RNA Structure Are Required for Efficient HCV Replication in Cultured Cells. PLoS Pathog 6(4): e1000885. doi:10.1371/journal.ppat.1000885

Editor: Michael Gale Jr., University of Washington, United States of America

Received October 21, 2009; **Accepted** March 30, 2010; **Published** April 29, 2010

Funding: A.M. is supported by the Japan Health Sciences Foundation and Viral Hepatitis Research Foundation of Japan. This work was supported by grants from the Chinese Academy of Sciences (O514P51131 and KSCX1-YW-10-03), the Chinese 973 project (2009CB522504) and the Chinese National Key Project (2008ZX1000Z-14) to T.T., and a grant-in-aid for Scientific Research from the Japan Society for the Promotion of Science, from the Ministry of Health, Labor and Welfare of Japan, and from the Ministry of Education, Culture, Sports, Science and Technology and by the Research on Health Sciences Focusing on Drug Innovation from the Japan Health Sciences Foundation to T.W. The funders had no role in study design, data collection and analysis, decision to publish, or preparation of the manuscript.

Competing Interests: The authors have declared that no competing interests exist.

* E-mail: wakita@nih.go.jp (TW); ttoyoda@sibs.ac.cn (TT)

☯ These authors contributed equally to this work.

Introduction

Hepatitis C virus (HCV) contains a positive-stranded RNA genome and belongs to the *Flaviviridae* family [1]. Chronic HCV infection affects more than 130 million people worldwide [2]. The HCV RNA genome is approximately 9.6 kb in length and contains a long open reading frame that encodes a polyprotein of approximately 3,010 amino acids. This polyprotein is processed into at least 10 polypeptides by host and viral proteases [3,4]. The 5'-untranslated region (UTR) contains a highly conserved internal ribosome entry site (IRES) that is 341 nucleotides long [5]. The 3'UTR is known to contain a variable region (VR), a poly pyrimidine "U/C" (polyU/UC) tract, and a 98-base X-region (3'X tail) [6]. The second stem loop of the X region interacts with the NS5BSL3 cis-acting replication element (CRE) and may contribute to initiation of negative strand RNA synthesis [7].

JFH-1 belongs to genotype 2a and is the only strain that can efficiently replicate and produce virions in HuH-7 and HuH-7-derived cell lines [8,9,10]. When the structural protein-coding regions of the non-replicating HCV strains were fused to the non-structural protein-coding region and 3'UTR of JFH-1, replication was initiated and virions were produced in HuH-7-derived cells [10,11]. In order to analyze the mechanisms underlying the robust replication of JFH-1, we compared JFH-1 with J6CF. J6CF shares approximately 90% sequence homology with JFH-1 but does not replicate in HuH-7 cells. Analysis of JFH-1/J6CF chimeras demonstrated that the NS3 helicase-coding region (N3H) and the NS5B-to-3'X (N5BX) region of JFH-1 conferred replication activity to J6CF in HuH-7 cells [12]. Mutations in the N3H region are expected to affect helicase activity, while mutations in the NS5B-to-3'X region may affect polymerase and replication activity through secondary or higher order structures of the RNA. We have also previously reported that JFH-1-type mutations in the NS5B region enhanced genotype 1b RdRP activity *in vitro* [13]. Thus, JFH-1-type mutations in the NS5B region of J6CF are hypothesized to enhance J6CF RdRP activity. As mentioned above, the 3'UTR of the HCV genome consists of a VR, polyU/UC tracts of various lengths and a highly conserved 3'X tail. Deletion of the VR was reported to allow replication in both cultured cells [14] and in the chimpanzee [15]. The

Author Summary

Hepatitis C virus (HCV) is a major cause of chronic liver disease. Chronic HCV infection affects more than 130 million people worldwide. An efficient cell culture system is indispensable for HCV research and the development of antiviral strategies, including antiviral drugs and vaccines. Using one HCV strain, JFH-1, we have developed a novel cell culture system that, for the first time, has allowed for both the production of infectious HCV and the analysis of the HCV life cycle. To date, JFH-1 is the only HCV strain that replicates efficiently in cultured cells. Understanding the mechanisms underlying replication of JFH-1 in cultured cells is important and advantageous for the development of antiviral strategies. In the present study, we demonstrate that high polymerase activity, enhanced kissing-loop interactions between the NS5B and 3′X regions, and optimal viral RNA structure of the 3′ UTR are required for the efficient replication of JFH-1 and viral production in cultured cells. Our data provides information that will prove essential for the establishment of replication-competent variants of HCV strains that are currently replication incompetent in cultured cells. This study also contributes to a better understanding of the mechanisms underlying persistent HCV infections.

minimum length of polyU/UC tract required for replication has also been previously determined [14,16].

In the current study, we examined RNA polymerase activity and the RNA structures of the NS5B and 3′UTR that contribute to HCV replication, and determined the essential domains required for robust HCV RNA replication in cultured cells.

Materials and Methods

Cell culture

HuH-7 cells [17] and Huh-7.5.1 cells [9] were cultured at 37°C in Dulbecco's modified Eagle's medium containing 10% fetal bovine serum under 5% CO_2 conditions.

Construction of plasmids encoding a C-terminal 12xHis tagged HCV RdRP lacking 21 C-terminal amino acids

HCV JFH-1 and J6CF RdRP without the C-terminal 21 amino acid hydrophobic sequence were PCR amplified from pJFH1 [8] and pJ6CF (a kind gift from Jens Bukh) [15], respectively. Primer sequences for mutagenesis are listed in Table S1. Following digestion with *Xba*I and *Xho*I, DNA fragments were cloned into the *Nhe*I and *Xho*I sites of pET21b (Novagen, Madison, WI), resulting in pET21bHCVJFH-1RdRpwt and pET21bHCVJ6-CFRdRpwt. pET21bHCVJFH-1RdRpwt and pET21bHCVJ6-CFRdRpwt were then digested with *Xba*I and *Xho*I and the RdRP fragments cloned into the same restriction sites of pET28a, resulting in pET21(KM)JFH-1RdRpwt and pET21(KM)J6CFR-dRpwt, respectively.

Mutation analysis of J6CF and JFH-1 RdRP

JFH-1-type substitutions (S377R, A450S, S455N, R517K, and Y561F in the NS5B region; amino acid numbers are based on the AA relative numbering [18]) were introduced into J6CF RdRP and J6CF-like substitutions (S450A, N455S, K517R, F561Y, and F561I) and D318A were introduced into JFH-1 RdRP using the QuickChange II Site-Directed Mutagenesis Kit (Stratagene, La Jolla, CA). Primer sequences for mutagenesis are listed in Table S1. Sequences were confirmed by nucleotide sequencing.

Expression, purification, and *in vitro* transcription of HCV RdRP

pET21(KM)JFH-1RdRPwt, pET21(KM)J6CFRdRPwt, and their mutants were expressed with pGEX-HSP90α [13] in *Escherichia coli* Rosetta/pLysS (Novagen). RdRP was then purified as previously described [13], with the exception that protein induction was undertaken at 18°C for 4 h. *In vitro de novo* transcription was performed as described previously [13]. Briefly, following 30 min pre-incubation without ATP, CTP, or UTP, 0.1 μM HCV RdRP was incubated in 50 mM Tris/HCl (pH 8.0), 200 mM monopotassium glutamate, 3.5 mM $MnCl_2$, 1 mM DTT, 0.5 mM GTP, 50 μM ATP, 50 μM CTP, 5 μM [α-^{32}P]UTP, 0.02 μM RNA template (SL12-1S) and 100 U/ml human placental RNase inhibitor at 29°C for 90 min. [^{32}P]-RNA products were subjected to PAGE (6% gel, 8 M urea). The resulting autoradiograph was analyzed with a Typhoon trio plus image analyzer (GE Healthcare, Piscataway, NJ). The radio isotope count of 184 nt RNA product of each mutant RdRPs was measured and compared to that of JFH-1 RdRP wt in the same PAGE.

Subgenomic-replicon constructs

pSGR-J6/N3H+5BSLX-JFH1/Luc was constructed by replacement of the 5BSL-to-3′X fragment (9211 to 9678 of JFH-1) generated by PCR with the corresponding fragment of pSGR-J6/N3H+3′UTR-JFH1/Luc [12]. Constructs with substitutions in NS5B region were generated as follows; mutations were introduced by PCR-based mutagenesis and *Xho*I-*Xba*I-restricted fragments were exchanged with the corresponding fragment of pSGR-J6/N3H+5BSLX-JFH1/Luc or pSGR-J6/N3H+3′UTR-JFH1/Luc [12]. To generate the constructs used for the analyses of the 3′UTR, VR fragments (9415–9479 of JFH-1 and J6CF) or polyU/UC fragments (9480–9579 of JFH-1 and 9480–9606 of J6CF) were generated by PCR and replaced with the corresponding fragment of pSGR-J6/N3H+5BSLX-JFH1/Luc. To generate the constructs with substitutions in the VR or 3′SL2, mutations were introduced by PCR-based mutagenesis and *Sgr*AI-*Xba*I-restricted fragments were exchanged with the corresponding fragment of pSGR-J6/N3H+5BSLX-JFH1/Luc. Primer sequences for mutagenesis are listed in Table S1.

Full-length genomic HCV constructs

Plasmids used in the analysis of genomic RNA replication and core production were constructed from pJ6/N3H+N5BX-JFH1 [12] and pJ6CF [15]. pJ6/N3H+5BSLX-JFH1 was constructed by replacement of the corresponding sequence with the 5BSL-to-3′X fragment (9211 to 9678 of JFH-1) generated by PCR. pJ6/N3H+3′UTR-JFH1 was constructed by using the N3H region [*Cla*I (3929) - *Eco*T22I (5293)] and 3′UTR [*Stu*I (9415) - *Xba*I (9678)] of JFH-1 to replace the corresponding sequences of pJ6CF. Mutagenesis was performed as described above.

RNA synthesis and transfection

RNA synthesis and transfection were performed as described previously [8,12]. Briefly, plasmids were linearized with *Xba*I, treated with Mung Bean Nuclease (New England Biolabs, Ipswich, MA) and purified. Linearized, purified DNA was then used as a template for *in vitro* RNA synthesis using the MEGAscript T7 kit (Ambion, Austin, TX) in accordance with the manufacturer's instructions. Synthesized RNA was treated with DNase I (Ambion) followed by purification using ISOGEN-LS (Nippon Gene, Tokyo, Japan). The quality of the synthesized RNA was examined via agarose gel electrophoresis. Ten micrograms of *in vitro*-

synthesized RNA was used for each electroporation. Trypsinized HuH-7 cells or Huh-7.5.1 cells (3×10^6 cells) were washed with Opti-MEM I (Invitrogen, Carlsbad, CA) and resuspended in Cytomix buffer [19]. RNA was then combined with 400 µl of cell suspension and the mixture was transferred to an electroporation cuvette (Bio-Rad, Hercules, CA). The cells were then pulsed at 260 V and 950 µF using the Gene Pulser II apparatus (Bio-Rad). Transfected cells were immediately transferred to 6-well plates containing culture medium and incubated at 37°C under standard 5% CO_2 conditions.

Luciferase reporter assay

Luciferase activity of the JFH-1 subgenomic replicon and chimeras in HuH-7 cells were measured as described previously [12,20]. Briefly, 5 µg of transcribed RNA was transfected into 3×10^6 HuH-7 cells by electroporation. Transfected cells were immediately resuspended in culture medium and seeded into 6-well culture plates. Cells were then harvested at 4, 24, and 48 h after transfection and lysed with 200 µl of Cell Culture Lysis Reagent (Promega, Madison, WI). Debris was removed by centrifugation. Luciferase activity was quantified using a Lumat LB9507 luminometer (EG & G Berthold, Bad Wildbad, Germany) and a Luciferase Assay System (Promega). Assays were performed three times independently, with each value corrected for transfection efficiency as determined by measuring luciferase activity 4 h after transfection. Data are presented as relative light units (RLU).

Quantification of HCV core protein

To estimate the concentration of HCV core protein in the culture medium, we harvested supernatants at the indicated time points. The supernatant was then passed through a filter with a 0.22- µm pore size (Millipore, Bedford, MA) and subjected to the chemiluminescence enzyme immunoassay (Lumipulse II HCV core assay, Fujirebio, Tokyo, Japan) in accordance with the manufacturer's instructions.

Infection of cells with secreted HCV and determination of infectivity

Culture medium from RNA transfected cells was collected at 72 hours post-transfection. Huh7.5.1 cells were seeded at a density of 1×10^4 cells per well in poly-*D*-lysine coated 96-well plates (CORNING, Corning, NY). On the following day, the collected culture media were serially diluted and used for inoculation of the seeded cells, and the plates were incubated for another 3 days at 37°C. The cells were fixed in methanol for 15 min at −20°C, and the infected foci were visualized by immunofluorescence as described below.

Cells were blocked for 1 hour with BlockAce (Dainippon Sumitomo Pharma, Osaka, Japan), then washed with PBS, followed by incubation with anti-core antibody at 50 µg/ml in BlockAce. After incubation for 1 hour at room temperature, the cells were washed and incubated with a 1:400 dilution of AlexaFluor 488-conjugated anti-mouse IgG (Molecular Probes, Eugene, OR) in BlockAce. The cells were then washed and examined using fluorescence microscopy (Olympus, Tokyo, Japan). Infectivity was quantified by counting the infected foci and expressed as focus forming units per milliliter (ffu/ml).

Chemicals and radio isotope

Nucleotides were purchased from GE, [α-^{32}P]UTP from New England Nuclear (Boston, MA), and human placental RNase inhibitor and restriction enzymes from TaKaRa (Shiga, Japan).

Statistical analysis

Significant differences were evaluated using the Student's *t*-test. $p<0.05$ was considered significant.

RNA secondary structure prediction

RNA secondary structure prediction was performed using Mfold software [21].

Results

As we have reported previously, the NS3 helicase and the NS5B-to-3′X regions of JFH-1 are important to confer replication competence to J6CF, a replication-incompetent strain [12]. Of these two regions, NS5B-to-3′X of JFH-1 is the most important to replication-competence. The NS5B region encodes RdRP, and the JFH-1-version of this polymerase may have high activity and be crucial to replication-competence. The requirement of 3′UTR of JFH-1 suggested that the RNA structure in this region is important for efficient genome replication. To understand the mechanisms of efficient replication of JFH-1 in HuH-7 cells, we focused on the NS5B-to-3′X region because the NS3 helicase region of JFH-1 had relatively minor effects on replication of J6CF derivatives [12]. In order to identify the important protein domains within RdRP required for efficient virus replication, we compared the RNA polymerase activity of HCV J6CF RdRP to that of JFH-1 RdRP using three assays, *in vitro* transcription with purified RdRP, *in vivo* virus RNA replication, and *in vivo* virus production. To identify the important sequences or structures in the NS5B-to-3′X region involved in efficient replication, we analyzed the effect of sequence differences in this region on replication of the viral genome.

Comparison of RNA polymerase activity *in vitro*

By comparing the sequence of RdRP of JFH-1 (GenBank Accession No. AB047639), J6CF (AF177036), other 2a strains (AB047640 – 5, AY746460, AF238481 - 5, AF169002 -5), a 1a strain (H77: AF009606), and four 1b strains (Con1: AJ238799, AB080299, AY045702, M58335), we found 14 amino acids variants unique to JFH-1 RdRP (57T, 130P, 131Q, 150A, 377R, 405I, 435V, 450S, 455N, 474M, 479H, 517K, 561F and 571S). We focused on five JFH-1-type amino acid substitutions (Q377R, A450S, S455N, R517K, and Y561F) that have been shown to increase the polymerase activity of 1b RdRP [13]. We introduced these JFH-1-type amino acid substitutions into J6CF RdRP, individually and in combination, to test their effects on polymerase activity. We also tested a J6CF RdRP variant with a R517K substitution because it was included in the J6/N3H+5BSLX-JFH1 replicon (see below), although it did not enhance the polymerase activity of 1b RdRP *in vitro* [13].

The RdRPs of HCV JFH-1 and J6CF and mutant variants were purified as indicated in the Materials and Methods and Fig. S1A. The polymerase activity of wild-type (wt) and mutant RdRPs was measured using a *de novo* transcription system (Fig. 1 and Fig. S1B). The activity of J6CF RdRP was 7.0±0.6% of that of JFH-1. Similar to results seen with 1b RdRP substitution variants, the single amino acid substitutions Q377R, A450S, S455N, R517K, and Y561F resulted in increased polymerase activity of J6CF RdRP (25.5±1.5, 27.7±1.0, 53.1±0.9, 16.9±3.5 and 16.7±2.5% of JFH-1 RdRP wt, respectively). However, combining double and triple amino acid substitutions did not demonstrate any additive or synergistic effects on the *in vitro* polymerase activity (Fig. 1).

JFH-1 RdRP variants with individual J6CF-type amino acid substitutions, including R377Q, S450A, N455S, K517R, and F561Y, were also examined *in vitro*. With the exception of N455S,

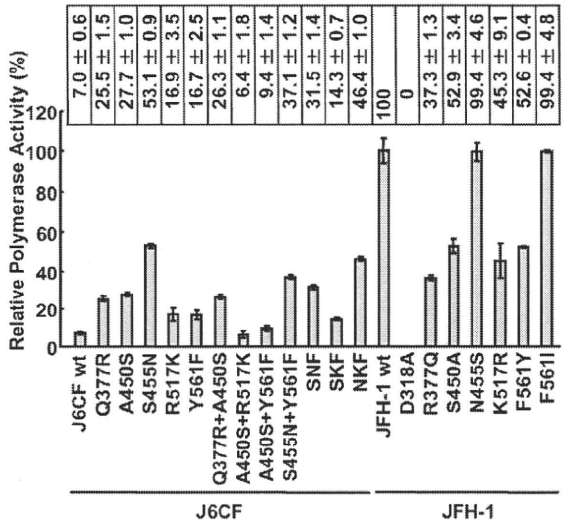

Figure 1. Relative HCV RNA polymerase activity of JFH-1 and J6CF wild-type and mutant RdRP. HCV RdRP activity was measured using the purified HCV RdRP (Fig. S1A) and the average RdRP activity and the standard deviation (error bar) relative to that of JFH-1 RdRP wt were calculated from three independent experiments (Representative gel images are shown in Fig. S1B). The relative activity values are presented above the graph. SNF, A450S+S455N+Y561F; SKF, A450S+R517K+Y561F; NKF, S455N+R517K+Y561F.
doi:10.1371/journal.ppat.1000885.g001

all other J6CF-type amino acid substitutions reduced the activity of JFH-1 RdRP, with levels ranging from 37.3 to 52.9% of the activity from wt JFH-1 RdRP (Fig. 1). The N455S variant maintained polymerase activity similar to that of JFH-1 wt. The JFH-1 D318A variant has a mutation in the active site of RdRP and showed no polymerase activity, confirming our *in vitro* transcription system.

JFH-1-type amino acid residues in the NS5B region restored the replication activity of the J6CF-based replicon

In order to test whether the JFH-1-type amino acids substitutions into the NS5B region of J6CF that enhanced polymerase activity *in vitro* enabled the replication of J6CF in cultured cells, we used the subgenomic J6CF replicon harboring the NS3 helicase region and 3′UTR of JFH-1 (J6/N3H+3′UTR-JFH1-Luc; Fig. 2A) as a reference construct. This replicon could replicate in cultured cells but exhibited less than 1% of the JFH-1 replication activity [12]. In order to test the effect of JFH-1 type amino acids on replication, we introduced the five substitutions that increased polymerase activity of J6CF RdRP *in vitro* (Q377R, A450S, S455N, R517K, and Y561F, see Fig. 2B) into the subgenomic replicon J6/N3H+3′UTR-JFH1-Luc and analyzed their effects on RNA replication. Among these JFH-1-type amino acids substitutions, Y561F was the most effective (23.2±3.5% of J6/N3H+N5BX-JFH1-Luc; Fig. 2C), while A450S, S455N, and R517K exhibited only a small effect on the replication activity (7.1±0.6%, 3.0±0.5%, and 5.5±1.0% of J6/N3H+N5BX-JFH1-Luc, respectively; Fig. 2C). The Q377R mutation demonstrated no effect on replication (Fig. 2C). We next tested the effects of Y561F in combination with each of the other substitutions. We found that A450S, S455N, and R517K mutations enhanced the replication activity of Y561F (59.1±6.1%, 43.9±6.6%, and 57.9±4.6% of J6/N3H+N5BX-JFH1-Luc, respectively; Fig. 2C). We also tested the effects of triple mutations and found that the replication activity of the SNF (A450S+S455N+Y561F) and SKF (A450S+R517K+Y561F) mutants demonstrated 86.8±6.0% and 112.2±7.9% replication activity of J6/N3H+N5BX-JFH1-Luc, respectively (Fig. 2C). In addition, we did not observe any significant differences between replicon activity of these mutants and that of J6/N3H+N5BX-JFH1-Luc. A combination of four mutations (SNKF; A450S+S455N+R517K+Y561F) resulted in similar activity as SKF (115.2±11.7% of J6/N3H+N5BX-JFH1-Luc; Fig. 2C). These results indicated that Y561F represented the most effective JFH-1-type mutation required for efficient replication, and that SKF and SNKF were sufficient to support replication activity equivalent to that of the replicon with the entire NS5B and 3′ UTR of JFH-1 (J6/N3H+N5BX-JFH1-Luc). The additive effects of the JFH-1-type NS5B substitutions on the replicon differed from results obtained with the *in vitro* polymerase activity assay.

Next, we examined whether these substitutions were sufficient for full-genome RNA replication and virus production. We used Huh-7.5.1 cells to assess virus production because Huh-7.5.1 is highly permissive for HCV propagation [9]. We found that J6/N3H+3′UTR-JFH1-Luc showed weak replication activity (Fig. 2C), and the core protein was not detectable in the culture medium of J6/N3H+3′UTR-JFH1-transfected cells (Fig. 3B). The constructs expressing A450S, S455N, or R517K substitution variants demonstrated only very low core levels in the supernatant, while the construct expressing the Y561F mutation underwent RNA replication and produced the core protein (Y561F; 15.5±3.0% of J6/N3H+N5BX-JFH1; Fig. 3B). Double mutants containing the Y561F mutation were found to produce greater amounts of core protein than the Y561F single mutant (A450S+Y561F, 57.4±3.3%; S455N+Y561F, 45.9±4.0%; and R517K+Y561F, 61.9±5.8% of J6/N3H+N5BX-JFH1; Fig. 3B). The triple mutant SNF (A450S+S455N+Y561F) produced more core protein than the double mutants (75.7±12.0% of J6/N3H+N5BX-JFH1; Fig. 3B). In addition, we observed that the core production from the SKF and SNKF mutant RNA-transfected cells was similar to the levels produced by J6/N3H+N5BX-JFH1 (111.5±8.8% and 119.0±5.1% of J6/N3H+N5BX-JFH1, respectively; Fig. 3B). We also measured infectivity of the supernatants from the mutant RNA-transfected cells at 72h after transfection (Fig. 3B). The levels of infectious titers correlated with the core levels among the tested constructs in this experiment. These results indicated that the SKF substitutions in the C-terminal region of NS5B were sufficient to elevate viral RNA replication and viral production.

Extra complementary sequence at the 5BSL3.2 kissing-loop interaction site of JFH-1 was essential for efficient replication

We observed a discrepancy between the *in vitro* RNA polymerase activity assay and the genome replication assay in the effects of the amino acid substitutions (Figs. 1 and 2C). Y561F was the most effective JFH-1-type amino acid substitution in the replication assay, while S455N was the most effective in the *in vitro* polymerase activity assay. As the kissing-loop interaction between 5BSL3.2 and 3′X are important for RNA replication and amino acid (aa) 561 encoding nucleotides are involved in the stem-loop 3.2 in the NS5B region (5BSL3.2) [7,16,22], we hypothesized that the cis-factor (genome structure) may also affect RNA replication in the cells. Thus, we constructed the subgenomic replicon J6/N3H+5BSLX-JFH1-Luc and the full genome construct J6/N3H+5BSLX-JFH1 that contained the NS3 helicase region and the 5BSL3-to-3′X region

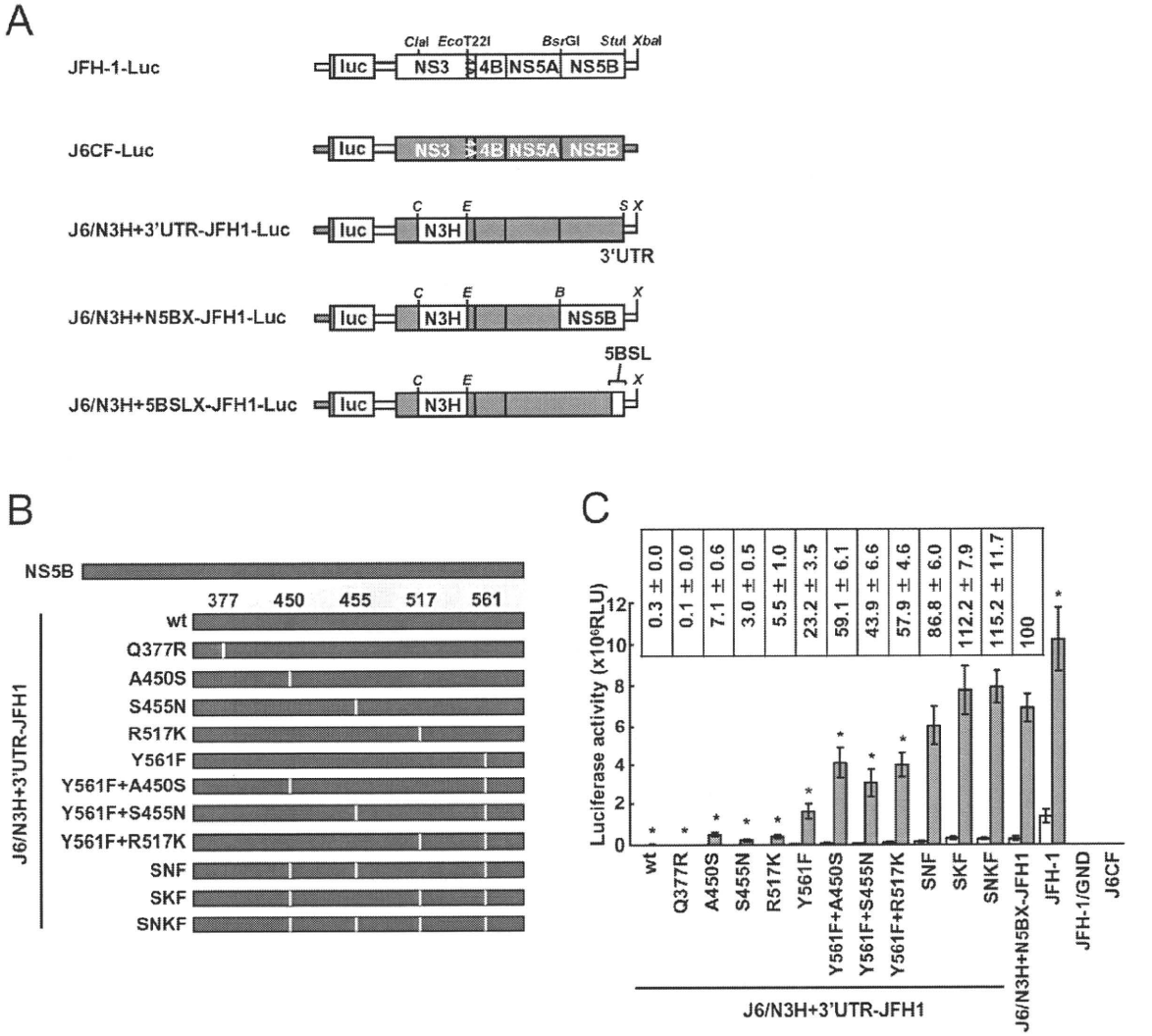

Figure 2. Luciferase activity of J6CF backbone replicons containing substitutions in the NS5B region. (A) Schematic structures of wt JFH-1 and J6CF constructs and the chimeric subgenomic replicons containing a J6CF backbone. The restriction enzyme recognition sites used for the construction of plasmids are indicated. *C*, *ClaI*; *E*, *EcoT22I*; *B*, *BsrGI*; *S*, *StuI*; *X*, *XbaI*; wt, wild-type. (B) Schematic diagram of the mutations introduced into J6/N3H+3'UTR-JFH1-Luc and J6/N3H+3'UTR-JFH1. (C) Replication activity of J6CF-based replicons. Subgenomic RNA was synthesized *in vitro* from wild-type or chimeric replicon constructs. Transcribed subgenomic RNA (5 μg) was then electroporated into HuH-7 cells and the cells harvested at 4, 24, and 48 h after transfection. The harvested cells were lysed, and the luciferase activity in the cell lysates was measured. The assays were performed three times independently and the results expressed as luciferase activities (RLU). Each value was corrected for transfection efficiency as determined by measuring the luciferase activity 4 h after transfection. Data are presented as the mean ± standard deviation for luciferase activity at 24 h (white bars) and 48 h (gray bars) after transfection. Asterisks indicate significant differences relative to the replication activity of J6/N3H+N5BX-JFH1 ($p<0.05$) at 48 h and the values represent the relative values against J6/N3H+N5BX-JFH1 at 48 h after transfection. SNF, A450S+S455N+Y561F; SKF, A450S+R517K+Y561F; SNKF, A450S+ S455N+R517K+Y561F.

doi:10.1371/journal.ppat.1000885.g002

(nucleotide (nt) 9211 to 9678) of JFH-1 (Figs. 2A and 3A), and determined their replication activity and virus production level. As presented in Figure 4B, the J6/N3H+5BSLX-JFH1-Luc construct demonstrated similar replication activity to that of J6/N3H+N5BX-JFH1-Luc 48h post-transfection (92.9±7.5% of J6/N3H+N5BX-JFH1; Fig. 4B). Moreover, both J6/N3H+N5BX-JFH1 and J6/N3H+5BSLX-JFH1 released similar levels of core protein into the supernatant (Fig. 3B).

We next analyzed the effects of mutations in the J6/N3H+5BSLX-JFH1 construct. The 5BSL region of this construct contains three amino acid differences from J6CF (R517K, Y561F, and L571S). R517K and Y561F were important in the *in vitro* polymerase activity assay (Fig. 1). We did not assess aa 571 *in vitro* because it was deleted to purify HCV RdRP. The replication activities of J6/N3H+5BSLX-JFH1-Luc with K517R or F561Y were found to be 28±2.7% and 14±2.0% of J6/N3H+5BSLX-JFH1-Luc, respectively, confirming the importance of these JFH-1-type amino acids for replication (Fig. 4B). J6/N3H+5BSLX-JFH1-Luc with S571L revealed similar replicon activity as the J6/N3H+5BSLX-JFH1-Luc (108±7.8% of J6/N3H+5BSLX-JFH1

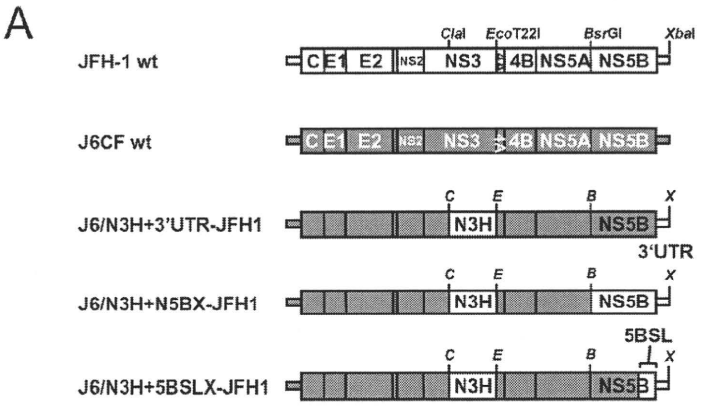

B

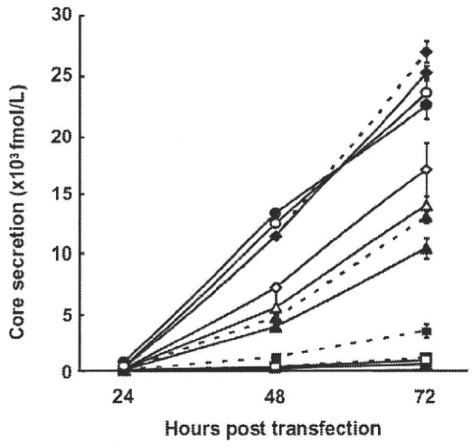

	Constructs	Core Secretion (%)	Infectivity (ffu/mL)
···◆···	SNKF	119.0 ± 5.1	$5.7x10^4$ ± $1.3x10^4$
—◆—	SKF	111.5 ± 8.8	$6.5x10^4$ ± $2.0x10^4$
—○—	J6/N3H+5BSLX-JFH1	104.7 ± 15.1	$5.8x10^4$ ± $4.7x10^3$
—●—	J6/N3H+N5BX-JFH1	100	$4.9x10^4$ ± $1.3x10^4$
—◇—	SNF	75.7 ± 12.0	$5.8x10^4$ ± $5.4x10^3$
—△—	R517K+Y561F	61.9 ± 5.8	$4.3x10^4$ ± $5.8x10^3$
···▲···	A450S+Y561F	57.4 ± 3.3	$2.6x10^4$ ± $6.9x10^3$
—▲—	S455N+Y561F	45.9 ± 4.0	$2.3x10^4$ ± $4.5x10^3$
···■···	Y561F	15.5 ± 3.0	$3.2x10^3$ ± $3.8x10^2$
—□—	R517K	4.2 ± 0.6	$7.0x10^1$ ± $1.0x10^1$
···□···	A450S	5.0 ± 0.1	$1.3x10^2$ ± $2.6x10^1$
—■—	S455N	2.7 ± 0.2	$1.4x10^2$ ± $3.1x10^1$
——	J6/N3H+3'UTR-JFH1	0.3 ± 0.1	$5.0x10^{-1}$ ± $0.0x10^0$

Figure 3. Analysis of transient replication of genomic chimeric HCV RNA. (A) The structure of full-length chimeric HCV RNA. Each chimeric full-length construct was prepared by the replacement of the indicated restricted fragments. The restriction enzyme recognition sites used for the plasmid constructions are indicated. *C*, *ClaI*; *E*, *Eco*T22I; *B*, *Bsr*GI; *S*, *StuI*; *X*, *XbaI*; wt, wild-type. (B) HCV core protein production in the culture medium from RNA-transfected cells. Transcribed wild-type or chimeric full-length HCV RNA (10 μg) was transfected into Huh-7.5.1 cells. Culture medium was harvested at 4, 24, 48, and 72 h after transfection. The amount of core protein in the harvested culture medium was measured using a HCV core chemiluminescence enzyme immunoassay (Lumipulse II HCV core assay). The assays were performed three times independently, and the data are presented as the mean ± standard deviation. Values in the right panel represent the relative core values against J6/N3H+N5BX-JFH1 at 72 h after transfection and infectious titers of the media from chimeric HCV RNA-transfected cells at 72h after transfection determined using Huh7.5.1 cells. SNF, A450S+S455N+Y561F; SKF, A450S+R517K+Y561F; SNKF, A450S+ S455N+R517K+Y561F.
doi:10.1371/journal.ppat.1000885.g003

wt; Fig. 4B). These results indicated the importance of 517K and 561F but not 571F in the 5BSL region of JFH-1 in efficient RNA replication. The codon encoding aa 561 possibly affects RNA structure, as it is located in the loop of stem-loop 3.2 in NS5B (5BSL3.2) and overlaps sequences important to the kissing-loop interaction with the stem loop 2 of the 3′X region (3′X SL2) [22]. Although we demonstrated that aa 561F was more effective than 561Y in RdRP activity *in vitro* (Fig. 1), it remains possible that the nucleotide mutation located at the codon of aa 561 affected the RNA structure and genome replication, as the replication activity of J6/N3H+3′UTR-JFH1-Luc with Y561F was the highest of all the clones with JFH-1 type single amino acids in the NS5B region (Fig. 2C). To investigate the effects of these mutations on RNA structure, we made mutants with nucleotide substitutions at the codon of aa 561 (Fig. 4F). The codon encoding aa 561 was UUU (Phe) for JFH-1 and UAU (Tyr) for J6CF. The third base of the codon overlaps with the kissing sequence [22]. In order to maintain the 5BSL3.2 stem loop structure and the kissing interaction between 5BSL3.2 and 3′X SL2, the third base should be U (nt 9349 of JFH-1). JFH-1 may exhibit additional interactions between 9348U of 5BSL3.2 and 9619A of 3′X SL2 to enhance kissing-loop interaction. To assess this hypothesis, we fixed the second base (9348) as U, and the first base (9347) was altered from U to A, G or C. The G and C substitutions were predicted to disrupt the important loop structure of 5BSL3.2 using Mfold and considered to affect replication activity. We next investigated the effects of U to A substitution (AUU, F561I) in an *in vitro* assay. F561I was introduced into JFH-1 RdRP and its RdRP activity was 99.4±4.8% of the wt, demonstrating that an F to I mutation did not affect polymerase activity (Fig. 1). We also examined the effects of the F561I mutation on RNA replication in the cells, and it revealed that it had similar replication activity as the wt,

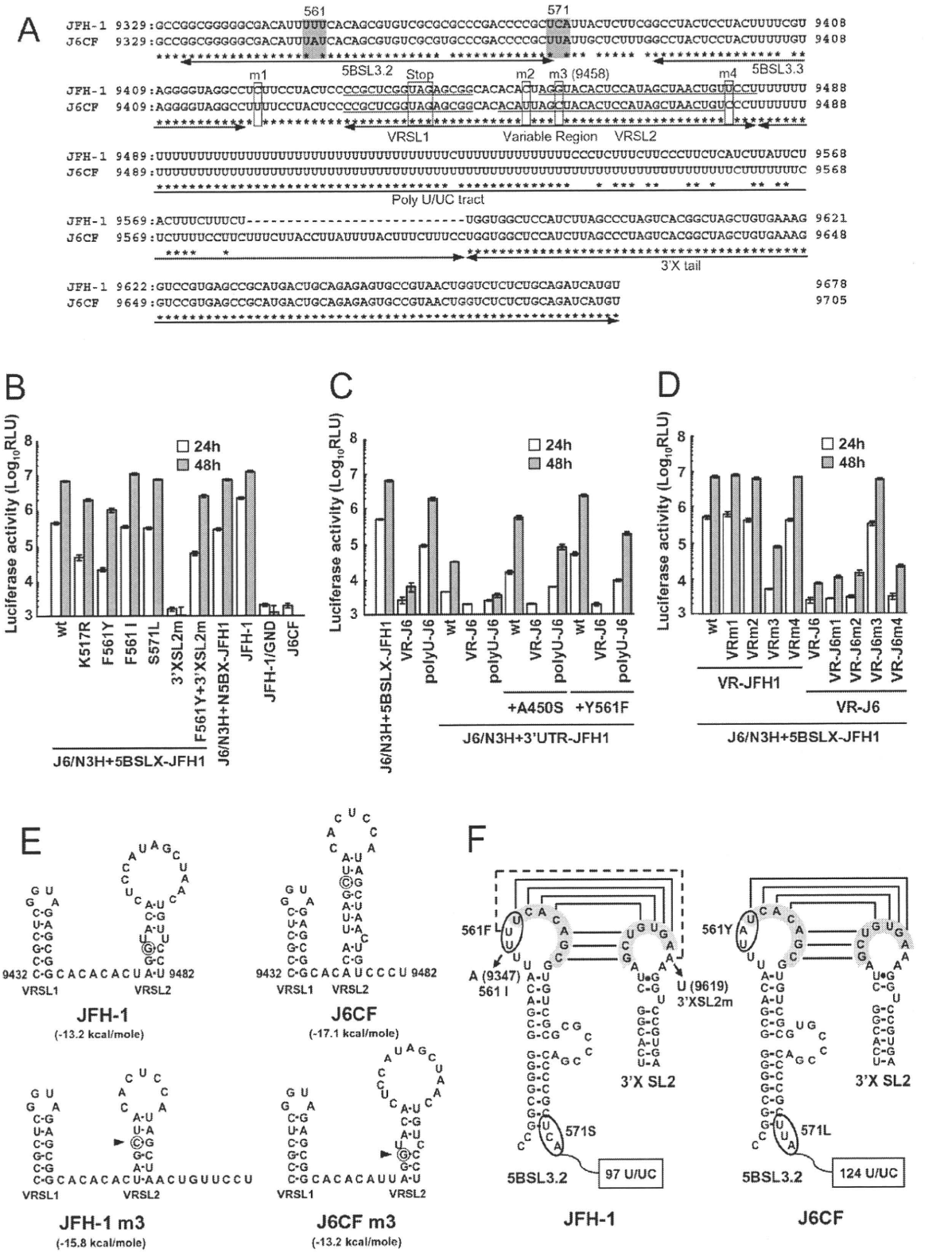
A
561
571
JFH-1 9329:GCCGGCGGGGGCGACAUUUUUCACAGCGUGUCGCGCGCCCGACCCCGCUCAUUACUCUUCGGCCUACUCCUACUUUUCGU 9408
J6CF 9329:GCCGGCGGGGGCGACAUUUAUCACAGCGUGUCGCGUGCCCGACCCCGCUUAUUGCUCUUUGGCCUACUCCUACUUUUUGU 9408
m1
5BSL3.2
Stop
m2
m3 (9458)
m4
5BSL3.3
JFH-1 9409:AGGGGUAGGCCUCUUCCUACUCCCCGCUCGGUAGAGCGGCACACACUAGGUACACUCCAUAGCUAACUGUCCCUUUUUUU 9488
J6CF 9409:AGGGGUAGGCCUUUUCCUACUCCCCGCUCGGUAGAGCGGCACACAUUAGCUACACUCCAUAGCUAACUGUCCCUUUUUUU 9488
VRSL1
Variable Region
VRSL2
JFH-1 9489:UUUUUUUUUUUUUUUUUUUUUUUUUUUUUUUUUUUUUUUUUUUUUUUUUUUUUUUUUUUUUUUUUUUUUUUUUUUU 9568
J6CF 9489:UUUUUUUUUUUUUUUUUUUUUUUUUUUUUUUUUUUUUUUUUUUUUUUUUUUUUUUUUUUUUUUUUUUUUUUUUUUUC 9568
Poly U/UC tract
JFH-1 9569:ACUUUCUUUCU----------UGGUGGCUCCAUCUUAGCCCUAGUCACGGCUAGCUGUGAAAG 9621
J6CF 9569:UCUUUUCCUUCUUUCUUACCUUAUUUUACUUUCUUUCCUGGUGGCUCCAUCUUAGCCCUAGUCACGGCUAGCUGUGAAAG 9648
3'X tail
JFH-1 9622:GUCCGUGAGCCGCAUGACUGCAGAGAGUGCCGUAACUGGUCUCUCUGCAGAUCAUGU 9678
J6CF 9649:GUCCGUGAGCCGCAUGACUGCAGAGAGUGCCGUAACUGGUCUCUCUGCAGAUCAUGU 9705
B
Luciferase activity (Log10RLU)
24h
48h
wt
K517R
F561Y
F561 I
S571L
3'XSL2m
F561Y+3'XSL2m
J6/N3H+N5BX-JFH1
JFH-1
JFH-1/GND
J6CF
J6/N3H+5BSLX-JFH1
C
Luciferase activity (Log10RLU)
24h
48h
J6/N3H+5BSLX-JFH1
VR-J6
polyU-J6
wt
VR-J6
polyU-J6
wt
VR-J6
polyU-J6
wt
VR-J6
polyU-J6
+A450S
+Y561F
J6/N3H+3'UTR-JFH1
D
Luciferase activity (Log10RLU)
24h
48h
wt
VRm1
VRm2
VRm3
VRm4
VR-J6
VR-J6m1
VR-J6m2
VR-J6m3
VR-J6m4
VR-JFH1
VR-J6
J6/N3H+5BSLX-JFH1
E
9432 C-G C A C A C A C U A-U 9482
VRSL1
VRSL2
JFH-1
(-13.2 kcal/mole)
9432 C-G C A C A U C C C U 9482
VRSL1
VRSL2
J6CF
(-17.1 kcal/mole)
C-G C A C A C U-A A C U G U U C C U
VRSL1
VRSL2
JFH-1 m3
(-15.8 kcal/mole)
C-G C A C A C A U U A-U
VRSL1
VRSL2
J6CF m3
(-13.2 kcal/mole)
F
561F
A (9347)
561 I
U (9619)
3'XSL2m
3'X SL2
571S
5BSL3.2
97 U/UC
JFH-1
561Y
3'X SL2
571L
5BSL3.2
124 U/UC
J6CF

Figure 4. Replication activity of J6CF-based replicons containing variants or substitutions. (A) Comparison of the nucleotide sequence of 5BSL3.2 to 3′X of JFH-1 and J6CF. Boxes indicate nucleotide differences in VR and stop codon. Shaded boxes indicate non-synonymous variants in this region. 5BSL3.2, 5BSL3.3, Variable Region (VR), Poly U/UC tract, and 3′X tail are indicated by double-headed arrows in the figure. Stem-loop structures of VR (VRSL1 and VRSL2) are underlined. Asterisk; conserved nucleotides between JFH-1 and J6CF. (B, C, D) Replication activity of J6CF-based replicons. Five micrograms of *in vitro* synthesized RNA was electroporated into HuH-7 cells and the cells were harvested at 4, 24, and 48 h after transfection. The harvested cells were then lysed, and the luciferase activity in the cell lysates was measured. The assays were performed three times independently, and the results were expressed as luciferase activities (RLU). Data are presented as the mean ± standard deviation for luciferase activity at 24 h (white bars) and 48 h (gray bars) after transfection. (E) The predicted secondary structure of the VR. The RNA secondary structures of JFH-1, JFH-1 m3, J6CF, and J6CF m3 were predicated by Mfold. The stem-loop structure 1 (VRSL1) and 2 (VRSL2) are indicated. Nucleotide 9458 is circled and the mutated nucleotides are indicated by arrowheads. (F) Schematic structures of the 5BSL3.2 and X tail. The predicted stem loop structure of 5BSL3.2 and SL2 of 3′X of JFH-1 and J6CF strains are indicated. The sequences forming kissing interaction with 3′X SL2 [22] are shaded. Codons encoding aa 561 and 571 are circled and the mutated sequences are indicated. The reported kissing-loop interactions are indicated by the connecting lines. The predicted interaction of the JFH-1 strain is indicated by the dotted connecting line.
doi:10.1371/journal.ppat.1000885.g004

confirming that this mutation exhibited no effect on RNA replication in cultured cells (Fig. 4B). These results demonstrated that both Phe and Ile could be substituted at aa 561 and revealed the importance of the precise RNA structure of this region. Finally, we introduced an A to U mutation at nt 9619 in the 3′X SL2 that was complementary to the second base of the codon encoding 561F (9348) to alter the kissing-loop interaction (Fig. 4F; 3′XSL2m). We observed a significant reduction in 3′XSL2m replication activity (Fig. 4B; 3′XSL2m). However, when 3′XSL2m was combined with the F561Y mutation that was expected to recover the kissing-loop interaction, replicon activity was restored (Fig. 4B; F561Y+3′XSL2m). These results indicated that the extra complementary sequence at the kissing-loop interaction site of 5BSL3.2 was important for the efficient RNA replication of JFH-1. The extra complementary sequence may enhance the kissing loop interactions. We also tested the effect of the Y561F substitution on replicons of other genotypes, H77S (GT1a) and HCV-N (GT1b). While the Y561F substitution increased replication activity in both genotype 1 strains (Text S1 and Fig. S3), the Y561F effect on the genotype 1 strains was much smaller than its corresponding effect on J6CF.

A shorter poly U/UC sequence in the JFH-1 strain favored replication

We next compared the sequences of the poly U/UC tracts of the 3′UTRs of JFH-1 and J6CF. The poly U/UC tract of JFH-1 was 27 nucleotides shorter than that of J6CF (Figs. 4A and F). The polyU stretch of the pJ6CF plasmid that we used was six nucleotides shorter than that of the original J6CF sequence reported ([15], GenBank: AF177036). In order to analyze the effects of poly U/UC length on HCV replication, the poly U/UC region of J6/N3H+5BSLX-JFH1-Luc was replaced with that of J6CF and was designated as polyU-J6. The replicon activity of J6/N3H+5BSLX-JFH1-Luc with polyU-J6 was approximately four times lower than that of the J6/N3H+5BSLX-JFH1-Luc (Fig. 4C). This result showed that longer polyU/UC region lengths of J6CF were not favorable for efficient replication.

JFH-1 type structure of the variable region was advantageous for efficient replication

When we compared the VR sequences of the 3′UTRs of JFH-1 and J6CF, we found that four nucleotides are different between the VRs of JFH-1 and J6CF and that substitution of the VR from JFH-1 with that of J6CF of J6/N3H+5BSLX-JFH1 resulted in a 1000-fold decrease in replication activity (Fig. 4C, VR-J6). Mfold analysis of predicted RNA secondary structure of the VR in JFH-1 and J6CF suggests that there are two stem-loop structures in the VR. The first stem loop (VRSL1) structure is identical in JFH-1 and J6CF, but the loop of the second stem-loop (VRSL2) is larger in JFH-1 than in J6CF (Fig. 4E). Analysis of the effects of these nucleotide mutations on RNA structure revealed that only the third mutation (m3 at 9458 in Fig. 4A) is predicted to alter the structure of VRSL2 (Fig. 4E). The m3 G substitution into J6CF VR generated a predicted structure identical to that of JFH-1 VRSL2 resulting in identical VR structures (Fig. 4E). The m3 C substitution altered the structure of JFH-1 VR to the J6CF type (Fig. 4E). Substitutions of other nucleotides did not change the predicted structures (Data not shown). We then analyzed the effects of the mutations on replication activity. The m3 C substitution in JFH-1 VR was found to reduce replication activity 100-fold of the J6/N3H+5BSLX-JFH1-Luc (Fig. 4D; VRm3), whereas other substitutions (Fig. 4A; m1, m2 and m4) did not reduce replication activity at all (Fig. 4D; VRm1, VRm2 and VRm4). In contrast, the construct containing the J6CF VR with m3 G substitution completely restored replication activity (Fig. 4D; VR-J6m3). Other JFH-1 type nucleotide did not restore replication activity (Fig. 4D; VR-J6m1, VR-J6m2 and VR-J6m4). These results were in agreement with the stem-loop structure prediction of VR (Fig. 4E), demonstrating that the JFH-1 VR increased RNA replication. These results suggested the importance of VR secondary structure. Next, we tested if the effect of VR of JFH-1 was restricted to NS5B of JFH-1 or not. We constructed replicons with NS5B of J6CF and tested the effect on replication. The replication activities of the replicon with entire NS5B of J6CF (J6/N3H+3′UTR-JFH1), J6/N3H+3′UTR-JFH1 with A450S or Y561F (J6/N3H+3′UTR-JFH1+A450S, J6/N3H+3′UTR-JFH1+Y561F, respectively) were enhanced by the VR of JFH-1 (see polyU-J6 of each constructs in Fig. 4C) and not enhanced by the VR of J6CF (see VR-J6 of each constructs in Fig. 4C). These results indicated that the VR structure of JFH-1 was preferable for both JFH-1- and J6CF-derived NS5B and this effect was independent of the enhanced kissing-loop interaction (compare J6/N3H+3′UTR-JFH1 wt and A450S vs. Y561F in Fig. 4C).

Discussion

It has been demonstrated previously that HCV JFH-1, the only strain that replicates and produces virions efficiently in cell culture systems, expresses high replication activity without adaptive mutations [8]. We have previously reported that the N3H and N5BX regions of JFH-1 were able to rescue replication of the genotype 2a replicons [12]. The NS3 helicase and N5BX regions have been shown to be important to the virus production in HuH-7 cells. We have continued this line of experiment in the current study by focusing on RdRP activity and the genome structure in the 5BSL3.2 (CRE) to 3′X region. Following these aims, we were able to define the amino acids, nucleotides, and structural elements of JFH-1 required to confer replication competence and replication efficiency to the closely related J6CF.

In the present study, we identified five JFH-1-type amino acid residues in NS5B (Q377R, A450S, S455N, R517K, and Y561F) important for HCV replication by the *in vitro* polymerase activity assay and *in vivo* assays using replicons and full length HCV RNA. These amino acid residues are all in the thumb domain of HCV RdRP. All of these JFH-1-type substitutions increased the polymerase activity of J6CF RdRP. J6CF-type amino acids substitution into JFH-1 RdRP, including R377Q, S450A, K517R, and F561Y, reduced polymerase activity, while the N455S substitution demonstrated similar activity to the JFH-1 wt. The A450S and S455N substitutions resulted in the most significant enhancement of 1b [13] and J6CF RdRP (Fig. 1), respectively. aa 450 is located at the tip of the β-hairpin, while aa 455 is located close to the lower portions of the β-hairpin that may control the entry of the RNA template [13]. Both the β-hairpin (aa 450 to 455) and the β-strand (aa 560 to 565) of the thumb domain play an important role in RNA binding due to their extensive hydrogen-bonding network [23]. The β-hairpin has been shown to prevent the recruitment of the primer-template complex into the RNA-binding site to ensure accurate initiation from the 3′ end of the template [24,25]. A450S and S455N are thought to possibly affect J6CF RdRP structure by changing the spacing of the nucleic acid binding pocket occluded by the β-hairpin. As JFH-1 N455S did not decrease the polymerase activity of JFH-1, the thumb domain of JFH-1 may be optimized to control the position or movement of the β-hairpin. Simister *et al.* have recently reported that the higher *in vitro* polymerase activity of JFH-1 was due to a higher *de novo* initiation efficiency that may be due to a closed conformation of the JFH-1 polymerase [26]. Eight amino acid mutations in NS5B of JFH-1 are hypothesized to be responsible for the conformational differences in the NS5B sequences JFH-1 and the 2a consensus [26]. However, these amino acids did not overlap with the mutations that we identified to be important for replication. Taken together, these two studies suggested that the thumb structure surrounding the β-hairpin is important to RdRP activity [26]. We only tested six of 29 amino acid differences and other mutations are possibly important to RdRP activity. However, SKF and SNKF slightly increased replication activity compared to the replicon with entire NS5B of JFH-1 (Fig. 2C). These results suggest that there may be some JFH-1-type variants in NS5B region that inhibit the replication activity of JFH-1. The JFH-1 and J6CF 5BSL regions (Fig. S2) differ in three amino acids. The JFH-1-type substitution R517K and Y561F increased replication, while the variation at aa 571 did not affect replication. This means that there are no JFH-1 variants in 5BSL region that inhibit replication activity. However, some other mutations which were not tested outside of 5BSL region may inhibit replication. Taken together, we considered that is why the replicon with 5BSLX of JFH-1 had almost the same replication activity as the replicon with entire NS5B region of JFH-1.

After comparing the activating effects of A450S and S455N vs. R517K and Y561F in the *in vitro* polymerase, *in vivo* RNA replication and virus production assays, we hypothesized that amino acids 517 and 561 likely control HCV genome replication via interactions with additional host and viral factors, including the NS3 helicase and 3′UTR. A450S enhances polymerase activity alone, while R517K and Y561F enhance genome transcription and replication activity via additional factors. The aa 455 and 517 are known to be located at the surface of the polymerase, and these mutations may affect interactions with the proteins that play important roles in RNA replication.

The combination of A450S, R517K, and Y561F substitutions conferred replication activity to the replicon with J6CF RdRP. The results of the core production were in agreement with the results from the replicon assay and suggested that these amino acid mutations affected only RNA replication and did not affect the additional steps in the virus life cycle within the cells, such as virus particle assembly and virus secretion.

We did, however, observe a discrepancy between the effects of the mutations on *in vitro* RNA polymerase activity and *in vivo* RNA replication and virus production activities. The S455N mutation conferred the highest levels of activity on J6CF RdRP *in vitro*, while Y561F conferred the highest replication and virus production activities on J6/N3H+3′UTR-JFH1 in the cells. We did not observe any combination effects of the substitutions in the *in vitro* polymerase assays, while strong combination effects of the substitutions were observed on replication and core production *in vivo*. In addition, the combination of only three substitutions (SKF; A450S, R517K, and Y561F) was enough to increase HCV replication to levels similar to that of the construct harboring both the entire NS5B region and the 3′UTR of JFH-1. We did not observe any combination effects of the substitutions in the *in vitro* polymerase assays using 1b RdRP [13]. However, a discrepancy between polymerase activity *in vitro* and replication activity was also reported for GTP binding site mutants [27].

Discrepancies between the results from *in vitro* polymerase activity assays and *in vivo* replication assays may arise because of differences in the assay systems. In an *in vitro* polymerase assay, only enzymatic activity can be determined, while an *in vivo* assay of replication activity does not necessarily represent the only polymerase activity. Many viral and host factors may be involved in the RNA replication step in the cells. If a HCV replication assay using entirely reconstituted components were possible, we could compare the isolated effect of different polymerase variants on polymerase activity.

In addition to RdRP activity, host and viral factors, including *cis*-acting RNA structures in the 3′-genome must be considered in HCV replication in cells. In fact, we found a JFH-1-type nucleotide variant in NS5B region important to maintain the genome structure in the *in vivo* assay; this *cis*-acting factor could not have been identified using the *in vitro* polymerase assay. The SKF triple substitution contains the 561F variant that is important for enhanced kissing-loop interaction and high polymerase activity, suggesting that the effects of the SKF combination *in vivo* are rather due to the enhanced kissing-loop interaction.

We also analyzed the 5BSL3.2 and 3′XSL2 structures required for kissing-loop interactions, as aa 561 is in the loop domain of 5BSL3.2 and the activation effect of Y561F in the *in vivo* replicon assay was larger than in the *in vitro* polymerase assay. In order to test the effects of JFH-1-type variants of 5BSL3.2 on replication, we substituted the amino acids located downstream of the 5BSL3-to-3′X region (nt 9211 to 9678) from JFH-1 into the J6CF construct carrying the JFH-1-type NS3 helicase (J6/N3H+5BSLX-JFH1). The J6/N3H+5BSLX-JFH1 exhibited similar replication and virus production levels to J6/N3H+N5BX-JFH1. We initially focused on the amino acid differences between JFH-1 and J6CF in the region spanning between JFH-1 5BSL-to-3′X because this region was able to complement the entire JFH-1 NS5B-to-3′ X region. We identified three amino acid differences (517, 561, and 571) in the 5BSLX regions of JFH-1 and J6CF. We then introduced J6CF-type substitutions into the 5BSL3.2 region of JFH-1 RdRP. The J6CF-type substitution in JFH-1 5BSL3.2 region at positions 517 and 561, but not 571, resulted in a reduction in replication. These findings were consistent with the results of the *in vitro* polymerase assay. RNA polymerase activity *in vitro* was analyzed using the ΔC21-molecule (1–570) and JFH-1 RdRP that did not contain 571S demonstrated high levels of polymerase activity, indicating that 571S may not be important for

its high polymerase activity. The codon encoding aa 517 is located outside of the 5BSL3.2 region, suggesting that this mutation only affected polymerase activity. The codon encoding aa 561 and aa 571 are within the 5BSL3.2 region. The codon encoding aa 561 is located within the loop of the 5BSL3.2, while the codon encoding aa 571 is in the spacer region located between 5BSL3.2 and 5BSL3.3. The nucleotide mutations resulting the K517R and S571L aa substitutions were predicted to maintain 5BSL3.2 RNA secondary structures similar to that of JFH-1 using Mfold analysis [21].

Since there was the possibility that Y561F mutation affected both RdRP protein activity and genomic RNA structures, we tested the effect of nucleotide substitutions in the aa 561 codon on replication. The third nucleotide (9349U) contained within the codon encoding aa 561 is conserved among the different genotypes and essential for the kissing-loop interaction [16,22]. The second nucleotide (nt 9348) of JFH-1 is a U, while that of J6CF an A. The first nucleotide (nt 9347) of the codon should be either an A or a U, because these nucleotides are required to maintain the loop structure. Thus, a Phe (JFH-1), Tyr (J6CF and 1b), or Ile (9347A) may reside at position 561. As JFH-1 RdRP F561I retained identical activity levels to the wt (561F), hydrophobic amino acids appeared to be required in this position to maintain the high polymerase activity. Since the predicted secondary structures of 5BSL3.2 were identical for JFH-1 and J6CF, both Phe located at position 561 and the nucleotide sequence UUU in JFH-1 were essential for the high replication activity in cultured cells.

The conserved sequences of the kissing-loop interaction were UCACAGC (nt 9349–9355) in 5BSL3.2 and GCUGUGA (nt 9612–9618) in 3′X SL2. In the case of JFH-1, the nucleotide located at position 9348 was U and the nucleotide located at position 9619 was A, resulting in extended kissing-loop interaction sequence in JFH-1. When we introduced a mutation into the 3′X SL2 region (nt 9619) that was expected to abolish the extra base pair next to the interaction site, replication activity was significantly decreased. In addition, a combination of the F561Y and 3′X SL2m substitutions, expected to restore the extra base pair between nt 9348 and nt 9619, restored replication. Replication level of this double substitution was slightly lower than that of the wt constructs, possibly due to the preference for Phe at 561 over Tyr for genome replication. Mfold analysis also revealed that RNA secondary structure was not affected following the introduction of these substitutions. U at nucleotide position 9348 was previously identified in various HCV strains registered in GenBank [7]. Taken together, these findings suggested that the strong kissing-loop interaction of the JFH-1 genome supports efficient genome replication in HuH-7 cells. We also tested the effect of Y561F substitution in two other genotypes, H77S (GT1a) and HCV-N (GT1b). While the Y561F substitution increased replication activity in both genotype 1 strains, the Y561F effect on the genotype 1 strains was much smaller than its corresponding effect on J6CF. These results may indicate that the levels of Y561F effect for viral RNA replication are different among the genotypes. These results may also indicate that the Y561F substitution enhanced replication of strains with a substantial replication capacity. In case of J6CF, the Y561F effect was only observed with N3H region and VR of JFH-1 (Fig. 4C, compare VR-J6 and polyU-J6 of J6/N3H+3′UTR-JFH1+Y561F). This result suggested that the Y561F effect was difficult to detect with replication-incompetent clones or clones with weak replication, and also suggested that other mutations or regions are important to replicate genotype 1 replicon efficiently. Therefore, we need more efficient replicating clone of genotype 1 to determine the effect and importance of this mutation on genotype 1 strains.

We next analyzed the effects of 3′UTR structure on replication and demonstrated that the polyU/UC of JFH-1 was 27 nucleotides shorter than that of J6CF. The shorter polyU/UC and the RNA structure of the VR of JFH-1 appeared enhance efficient replication. When using the activated RdRP (SKF) and the optimal RNA structure of the 3′ genome together with the JFH-1 NS3 helicase, we found that J6CF, which did not replicate in cells, was successfully converted to a replicating virus. The VR sequence is generally not conserved, even among strains within the same genotype, and the effects of VR on HCV replication remain controversial [14,15,28]. Our data revealed that the VR of JFH-1 was more favorable than that of J6CF for replication. Substitution of the VR from JFH-1 to J6CF significantly reduced replication levels 1000-fold. This dramatic change in replication activity was likely due to alterations in the RNA structure with a mutation at nt 9458. The predicted RNA structure of the VR and replication activity of the constructs containing substitutions or mutations to the VR were completely correlated. It is therefore very likely that cellular and viral factors interact with the HCV genome in this region, and that the specific nucleotide sequence and higher structure of the VR may be essential for these interactions. There is a possibility of genetic interaction between the VR and NS5B region. These kinds of interaction may also affect on polymerase activity.

The length of the polyU/UC tract appeared to be flexible and even differed within the same genotype. Even though JFH-1 and J6CF shared an identical 3′X, the JFH-1 poly U/UC tract (nt 9483–nt 9579) was 27 U shorter than that of J6CF (nt 9483–nt 9606). Thus, we examined whether the polyU/UC tract could be exchanged between JFH-1 and J6CF. The J6/N3H+5BSLX-JFH1 variant that contained the J6CF polyU/UC exhibited a four-fold reduction in replication, demonstrating that the polyU/UC did indeed affect replication. Several published papers have investigated the affects of length on the polyU/UC region [14,15,16]. Several viral and cellular proteins have also been reported to interact with the polyU sequence [29,30,31,32,33,34,35,36]. The preferential length and nucleotide sequence of the polyU/UC may be determined by interaction with these factors.

In conclusion, we found that high RdRP activity, enhanced kissing-loop interaction between 5BSL3.2 and 3′X SL2, optimal VR structure and a shorter polyU/UC tract in JFH-1 contributed to the high levels of HCV RNA replication and virus production in cultured cells. As NS3 helicase region of JFH-1 is also important for replication and viral production of J6CF, the replication enhancing mechanism of NS3 helicase region should be analyzed.

Supporting Information

Figure S1 (A). Purified HCV J6CF and JFH-1 mutant RNA polymerases. HCV RdRp variants were purified as indicated in the Materials and Methods section. Five pmol of RdRp were applied on 10% SDS-PAGE and stained with Coomassie brilliant blue. The designations of HCV J6CF and JFH-1 wt and mutants are indicated above the PAGE. M; molecular weight marker (Takara), and the position is indicated on the left. (B). Representative PAGE of *in vitro* transcription of HCV J6CF and JFH-1 mutant RNA polymerases. *In vitro de novo* transcription was performed as indicated in the Materials and Method section. [^{32}P]-RNA products were applied on 6% PAGE containing 8 M urea. The autoradiography was analyzed by Typhoon trio plus image analyzer. The radio isotope count of 184 nt RNA product was measured and compared to that of JFH-1 RdRp wt in the same PAGE. The designations of HCV J6CF and JFH-1 wt and mutants are indicated above the PAGE. M; [^{32}P]-25 base DNA

ladder (Takara), and the position is indicated on the left. The position of 184 nt RNA product is indicated on the right.
Found at: doi:10.1371/journal.ppat.1000885.s001 (0.45 MB TIF)

Figure S2 Comparisons of the amino acid sequence of NS5B of JFH-1 and J6CF. The 5BSL region is indicated with a box.
Found at: doi:10.1371/journal.ppat.1000885.s002 (0.13 MB TIF)

Figure S3 Effect of Y561F substitution on replication activity of genotype 1 replicons. Replication activity of genotype 1a (H77S:(A)) and 1b (HCV-N:(B)) replicons. Subgenomic RNA was synthesized *in vitro* from wild-type or chimeric replicon constructs. Transcribed subgenomic RNA (5 μg) was then electroporated into HuH-7 cells and the cells serially harvested 4, 24, and 48 h after transfection. The harvested cells were lysed and the luciferase activity of the cell lysates was measured. The assays were performed three times independently, and the results expressed as luciferase activities (RLU). Luciferase activity is expressed as the change in RLU (n-fold) relative to the luciferase activity 4 h after transfection. Each value was corrected for transfection efficiency as determined by measuring the luciferase activity 4 h after transfection. Data are presented as the mean ± standard deviation for luciferase activity.
Found at: doi:10.1371/journal.ppat.1000885.s003 (0.08 MB TIF)

Table S1 Oligonucleotides used for construction.
Found at: doi:10.1371/journal.ppat.1000885.s004 (0.04 MB XLS)

Text S1 Supplementary materials and methods
Found at: doi:10.1371/journal.ppat.1000885.s005 (0.03 MB DOC)

Acknowledgments

We thank Y. Gao for her technical assistance. The pJ6CF plasmid was kindly provided by Jens Bukh. The pCVH77c plasmid was kindly provided by Robert H. Purcell. The pFKI389/neo/NS3-3′/wt plasmid was kindly provided by Ralf Bartenschlager. The pH77-S, pNNeo/3-5B, and pNNeo/3-5BΔGDD plasmids were kindly provided by Stanley M. Lemon.

Author Contributions

Conceived and designed the experiments: AM LW XT TS TK TW TT. Performed the experiments: AM LW XT. Analyzed the data: AM LW XT TS TK TW TT. Contributed reagents/materials/analysis tools: TD DA YT MM. Wrote the paper: AM LW TW TT.

References

1. Lemon S, Walker C, Alter M, Yi M (2007) Hepatitis C virus. In: Knipe D, Howley P, eds. Fields Virology 5 ed. PhiladelphiaPA: Lippincott-Raven Publishers. pp 1253–1304.
2. Wasley A, Alter MJ (2000) Epidemiology of hepatitis C: geographic differences and temporal trends. Semin Liver Dis 20: 1–16.
3. Grakoui A, Wychowski C, Lin C, Feinstone SM, Rice CM (1993) Expression and identification of hepatitis C virus polyprotein cleavage products. J Virol 67: 1385–1395.
4. Hijikata M, Mizushima H, Tanji Y, Komoda Y, Hirowatari Y, et al. (1993) Proteolytic processing and membrane association of putative nonstructural proteins of hepatitis C virus. Proc Natl Acad Sci U S A 90: 10773–10777.
5. Tsukiyama-Kohara K, Iizuka N, Kohara M, Nomoto A (1992) Internal ribosome entry site within hepatitis C virus RNA. J Virol 66: 1476–1483.
6. Tanaka T, Kato N, Cho MJ, Shimotohno K (1995) A novel sequence found at the 3′ terminus of hepatitis C virus genome. Biochem Biophys Res Commun 215: 744–749.
7. You S, Stump DD, Branch AD, Rice CM (2004) A cis-acting replication element in the sequence encoding the NS5B RNA-dependent RNA polymerase is required for hepatitis C virus RNA replication. J Virol 78: 1352–1366.
8. Wakita T, Pietschmann T, Kato T, Date T, Miyamoto M, et al. (2005) Production of infectious hepatitis C virus in tissue culture from a cloned viral genome. Nat Med 11: 791–796.
9. Zhong J, Gastaminza P, Cheng G, Kapadia S, Kato T, et al. (2005) Robust hepatitis C virus infection in vitro. Proc Natl Acad Sci U S A 102: 9294–9299.
10. Lindenbach BD, Evans MJ, Syder AJ, Wolk B, Tellinghuisen TL, et al. (2005) Complete replication of hepatitis C virus in cell culture. Science 309: 623–626.
11. Pietschmann T, Kaul A, Koutsoudakis G, Shavinskaya A, Kallis S, et al. (2006) Construction and characterization of infectious intragenotypic and intergenotypic hepatitis C virus chimeras. Proc Natl Acad Sci U S A 103: 7408–7413.
12. Murayama A, Date T, Morikawa K, Akazawa D, Miyamoto M, et al. (2007) The NS3 helicase and NS5B-to-3′X regions are important for efficient hepatitis C virus strain JFH-1 replication in Huh7 cells. J Virol 81: 8030–8040.
13. Weng L, Du J, Zhou J, Ding J, Wakita T, et al. (2009) Modification of hepatitis C virus 1b RNA polymerase to make a highly active JFH1-type polymerase by mutation of the thumb domain. Arch Virol 154: 765–773.
14. Friebe P, Bartenschlager R (2002) Genetic analysis of sequences in the 3′ nontranslated region of hepatitis C virus that are important for RNA replication. J Virol 76: 5326–5338.
15. Yanagi M, Purcell RH, Emerson SU, Bukh J (1999) Hepatitis C virus: an infectious molecular clone of a second major genotype (2a) and lack of viability of intertypic 1a and 2a chimeras. Virology 262: 250–263.
16. You S, Rice CM (2008) 3′ RNA elements in hepatitis C virus replication: kissing partners and long poly(U). J Virol 82: 184–195.
17. Nakabayashi H, Taketa K, Miyano K, Yamane T, Sato J (1982) Growth of human hepatoma cells lines with differentiated functions in chemically defined medium. Cancer Res 42: 3858–3863.
18. Kuiken C, Combet C, Bukh J, Shin IT, Deleage G, et al. (2006) A comprehensive system for consistent numbering of HCV sequences, proteins and epitopes. Hepatology 44: 1355–1361.
19. van den Hoff MJ, Moorman AF, Lamers WH (1992) Electroporation in 'intracellular' buffer increases cell survival. Nucleic Acids Res 20: 2902.
20. Kato T, Date T, Miyamoto M, Sugiyama M, Tanaka Y, et al. (2005) Detection of anti-hepatitis C virus effects of interferon and ribavirin by a sensitive replicon system. J Clin Microbiol 43: 5679–5684.
21. Zuker M (2003) Mfold web server for nucleic acid folding and hybridization prediction. Nucleic Acids Res 31: 3406–3415.
22. Friebe P, Boudet J, Simorre JP, Bartenschlager R (2005) Kissing-loop interaction in the 3′ end of the hepatitis C virus genome essential for RNA replication. J Virol 79: 380–392.
23. Leveque VJ, Johnson RB, Parsons S, Ren J, Xie C, et al. (2003) Identification of a C-terminal regulatory motif in hepatitis C virus RNA-dependent RNA polymerase: structural and biochemical analysis. J Virol 77: 9020–9028.
24. Zhong W, Ferrari E, Lesburg CA, Maag D, Ghosh SK, et al. (2000) Template/primer requirements and single nucleotide incorporation by hepatitis C virus nonstructural protein 5B polymerase. J Virol 74: 9134–9143.
25. Hong Z, Cameron CE, Walker MP, Castro C, Yao N, et al. (2001) A novel mechanism to ensure terminal initiation by hepatitis C virus NS5B polymerase. Virology 285: 6–11.
26. Simister P, Schmitt M, Geitmann M, Wicht O, Danielson UH, et al. (2009) Structural and functional analysis of hepatitis C virus strain JFH1 polymerase. J Virol.
27. Cai Z, Yi M, Zhang C, Luo G (2005) Mutagenesis analysis of the rGTP-specific binding site of hepatitis C virus RNA-dependent RNA polymerase. J Virol 79: 11607–11617.
28. Arumugaswami V, Remenyi R, Kanagavel V, Sue EY, Ngoc Ho T, et al. (2008) High-resolution functional profiling of hepatitis C virus genome. PLoS Pathog 4: e1000182. doi:10.1371/journal.ppat.1000182.
29. Kanai A, Tanabe K, Kohara M (1995) Poly(U) binding activity of hepatitis C virus NS3 protein, a putative RNA helicase. FEBS Lett 376: 221–224.
30. Luo G, Hamatake RK, Mathis DM, Racela J, Rigat KL, et al. (2000) De novo initiation of RNA synthesis by the RNA-dependent RNA polymerase (NS5B) of hepatitis C virus. J Virol 74: 851–863.
31. Huang L, Hwang J, Sharma SD, Hargittai MR, Chen Y, et al. (2005) Hepatitis C virus nonstructural protein 5A (NS5A) is an RNA-binding protein. J Biol Chem 280: 36417–36428.
32. Gontarek RR, Gutshall LL, Herold KM, Tsai J, Sathe GM, et al. (1999) hnRNP C and polypyrimidine tract-binding protein specifically interact with the pyrimidine-rich region within the 3′NTR of the HCV RNA genome. Nucleic Acids Res 27: 1457–1463.
33. Luo G (1999) Cellular proteins bind to the poly(U) tract of the 3′ untranslated region of hepatitis C virus RNA genome. Virology 256: 105–118.
34. Petrik J, Parker H, Alexander GJ (1999) Human hepatic glyceraldehyde-3-phosphate dehydrogenase binds to the poly(U) tract of the 3′ non-coding region of hepatitis C virus genomic RNA. J Gen Virol 80 (Pt12): 3109–3113.
35. Spangberg K, Wiklund L, Schwartz S (2001) Binding of the La autoantigen to the hepatitis C virus 3′ untranslated region protects the RNA from rapid degradation in vitro. J Gen Virol 82: 113–120.
36. Spangberg K, Wiklund L, Schwartz S (2000) HuR, a protein implicated in oncogene and growth factor mRNA decay, binds to the 3′ ends of hepatitis C virus RNA of both polarities. Virology 274: 378–390.

GASTROENTEROLOGY 2010;139:1355–1364

BASIC—LIVER, PANCREAS, AND BILIARY TRACT

Production of Infectious Hepatitis C Virus in Primary Cultures of Human Adult Hepatocytes

PHILIPPE PODEVIN,* ARNAUD CARPENTIER,*,‡ VÉRONIQUE PÈNE,* LYNDA AOUDJEHANE,‡ MATTHIEU CARRIÈRE,‡ SAKINA ZAÏDI,* CÉLINE HERNANDEZ,* VANESSA CALLE,* JEAN-FRANÇOIS MÉRITET,*,§ OLIVIER SCATTON,‖ MARLÈNE DREUX,¶ FRANÇOIS-LOÏC COSSET,¶ TAKAJI WAKITA,# RALF BARTENSCHLAGER,** SYLVIE DEMIGNOT,‡‡ FILOMÉNA CONTI,‡ ARIELLE R. ROSENBERG,*,§ and YVON CALMUS‡

*INSERM, Equipe Avenir "Virologie de l'Hépatite C," Institut Cochin, Paris, France; ‡Université Paris Descartes, UPRES 1833, Paris, France; §Université Paris Descartes; AP-HP, Groupe Hospitalier Cochin, Service de Virologie, Paris, France; ‖AP-HP, Groupe Hospitalier Cochin, Service de Chirurgie, Paris, France; ¶INSERM, U 758; IFR 128, Biosciences Lyon-Gerland; Ecole Normale Supérieure de Lyon, Department of Human Virology, Lyon, France; #National Institute of Infectious Diseases, Department of Virology II, Tokyo, Japan; **University of Heidelberg, Department of Molecular Virology, Heidelberg, Germany; ‡‡INSERM; Université Pierre et Marie Curie; Université Paris Descartes; Centre de Recherche des Cordeliers, UMRS 872; EPHE, Laboratoire de Pharmacologie Cellulaire et Moléculaire, Paris, France

See editorial on page 1090.

BACKGROUND & AIMS: Although hepatitis C virus (HCV) can be grown in the hepatocarcinoma-derived cell line Huh-7, a cell-culture model is needed that supports its complete, productive infection cycle in normal, quiescent, highly differentiated human hepatocytes. We sought to develop such a system. **METHODS:** Primary cultures of human adult hepatocytes were inoculated with HCV derived from Huh-7 cell culture (HCVcc) and monitored for expression of hepatocyte differentiation markers and replication of HCV. Culture supernatants were assayed for HCV RNA, core antigen, and infectivity titer. The buoyant densities of input and progeny virus were compared in iodixanol gradients. **RESULTS:** While retaining expression of differentiation markers, primary hepatocytes supported the complete infectious cycle of HCV, including production of significant titers of new infectious progeny virus, which was called *primary-culture–derived virus* (HCVpc). Compared with HCVcc, HCVpc had lower average buoyant density and higher specific infectivity; this was similar to the characteristics of virus particles associated with the very-low-density lipoproteins that are produced during in vivo infection. These properties were lost after re-culture of HCVpc in poorly differentiated Huh-7 cells, suggesting that authentic virions can be produced only by normal hepatocytes that secrete authentic very-low-density lipoproteins. **CONCLUSIONS: We have established a cell-culture–based system that allows production of infectious HCV in physiologically relevant human hepatocytes. This provides a useful tool for the study of HCV interactions with its natural host cell and for the development of antiviral therapies.**

Keywords: Antiviral Drug Assay; Cell Permissiveness; Hepatocellular Physiology; Virus Propagation.

Hepatitis C virus (HCV) is a leading cause of chronic liver disease worldwide. This positive-strand RNA virus was identified by molecular cloning in 1989, and classified into 7 genotypes within its own genus. Twenty years later, however, the only approved treatment, pegylated interferon-alfa combined with ribavirin, is far from being fully satisfactory, hence there is a clear need for a better understanding of the virus life cycle and the rational development of novel therapies to interrupt it.[1] The availability of relevant cell-culture–based models is essential to achieve these goals, but culturing HCV has turned out to be a notoriously difficult task.[2,3] Because replication of this virus in vivo occurs mainly in highly differentiated, nondividing hepatocytes, primary cultures of human adult hepatocytes (PHH)[4] provide the closest in vitro model for the natural host cell of HCV. However, despite numerous attempts to infect PHH using sera from HCV-infected patients as sources of virus, replication of the viral genome was difficult to detect and production of measurable titers of progeny virus has not been achieved.[5–9] Accordingly, uncertainties persist as to whether these PHH-based systems faithfully reflect pro-

Abbreviations used in this paper: ApoB, apolipoprotein B; CYP, cytochrome P450; ffu, focus-forming units; HCVcc, hepatitis C virus derived from culture in Huh-7 cell line; HCVpc, hepatitis C virus derived from primary culture of human adult hepatocytes; HCVrecc, hepatitis C virus derived from re-culture in the Huh-7 cell line of hepatitis C virus derived from primary culture of human adult hepatocytes; MOI, multiplicity of infection; NS3, HCV nonstructural protein 3; PHH, primary human adult hepatocytes; VLDL, very-low-density lipoprotein.

0016-5085/$36.00
doi:10.1053/j.gastro.2010.06.058